water

MDPI

Supplementary Material

Assessing the Impact of Cyanuric Acid on Bather's Risk of Gastrointestinal Illness at Swimming Pools

Richard A. Falk [1,*], Ernest R. Blatchley III [2], Thomas C. Kuechler [3], Ellen M. Meyer [4], Stanley R. Pickens [5] and Laura M. Suppes [6]

S1. Steady-State Turbulent Diffusion Model of Pathogen Risk

A detailed diagram of the model inputs, intermediate calculated parameters, and results is presented in Figure S1. The dark yellow ovals are input parameters (light yellow are indirect input parameters set automatically via pulldown menus for pathogen selection and age of shedder), and cyan, orange, and purple ovals are calculated parameters that appear in more than one place in the diagram so are connections to have the diagram fit into a single page.

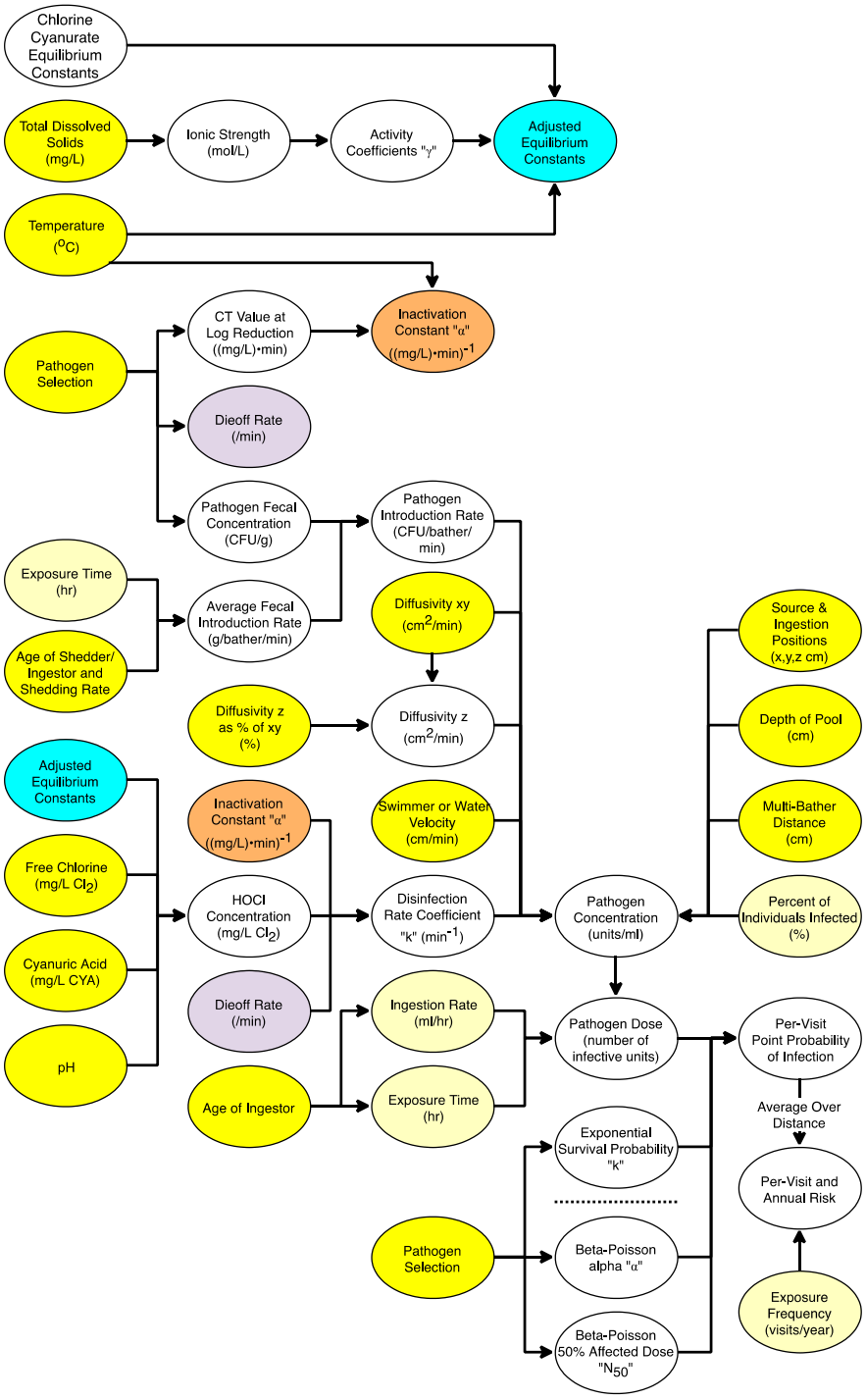

Figure S1. Detailed model diagram.

S2. Calculating HOCl Concentration from Cyanurate Chemistry

Cyanuric acid (CYA) readily converts between two tautomers, as indicated in Figure S2. The enol form predominates for unchlorinated cyanuric acid in the solid state. In solution or when

chlorinated, the keto form (isocyanuric acid) dominates. For the sake of simplicity, cyanuric acid (or isocyanuric acid) is represented as H_3Cy in the rest of this addendum.

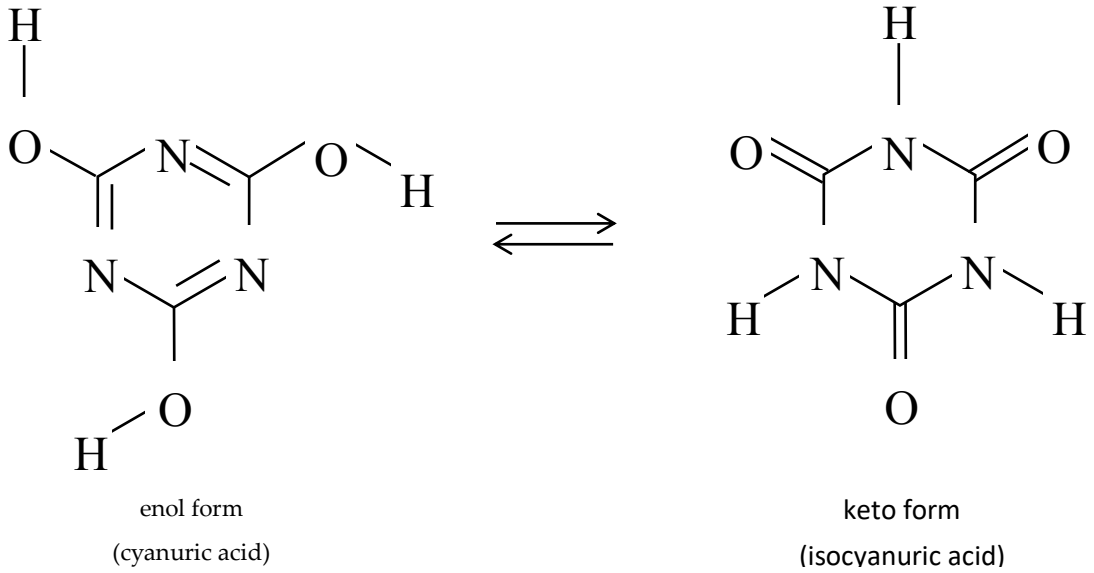

Figure S2. Two tautomers of cyanuric acid.

The three protons on the cyanuric acid ring can be sequentially removed at increasing pH to produce mono-negative, di-negative, and tri-negative anions. Alternatively, each of the three hydrogens can be replaced with a chlorine in a formal +1 oxidation state to form monochloro-, dichloro-, or trichloro-isocyanuric acid.

There are three possible deprotonation (acid dissociation) reactions associated with cyanuric acid. In addition, there are two deprotonation reactions possible for the monochloroisocyanuric acid and a single deprotonation reaction possible for dichloroisocyanuric acid. This gives rise to six independent equilibrium reactions and the corresponding equilibrium equations.

In Table S1, reactions (S1) through (S6) are acid deprotonation reactions associated with cyanurate species. The corresponding equilibrium Equations (S1) through (S6) along with the numeric values of the equilibrium constants are provided on the same rows of the table. Reactions and Equations (S7) through (S9) relate to the three hydrolysis reactions for chlorinated cyanurate forms. Finally, reaction (S10) is the acid dissociation (or deprotonation) of hypochlorous acid.

In the current work, the equilibrium constants shown in the table were adjusted to allow for the impact of ionic strength on activity coefficients so that concentrations rather than activities could be plugged into the equations. Ionic strength corrections are discussed in Section S3. In some cases, the equilibrium constants were also adjusted for temperature. Omitted from the table are redundant equilibrium constants, which can be determined from related constants listed in the table. For instance, the value of $K_{HClCy^-,h} = [H_2Cy^-]\cdot[HOCl]/[HClCy^-]$ can be determined from Equations (S1), (S4), and (S7): $K_{HClCy^-,h} = K_{H3Cy,a} \cdot K_{H2ClCy,h} / K_{H2ClCy,a}$.

Table S1. Acid dissociation reactions and equilibrium constants related to cyanuric acid. [1]

#	Equilibrium Reaction	Equation
(S1)	$H_3Cy \rightleftharpoons H^+ + H_2Cy^-$	$K_{H_3Cy,a} = \frac{[H^+]\cdot[H_2Cy^-]}{[H_3Cy]} = 1.3 \times 10^{-7}$
(S2)	$H_2Cy^- \rightleftharpoons H^+ + HCy^{2-}$	$K_{H_2Cy^-,a} = \frac{[H^+]\cdot[HCy^{2-}]}{[H_2Cy^-]} = 4 \times 10^{-12}$
(S3)	$HCy^{2-} \rightleftharpoons H^+ + Cy^{3-}$	$K_{HCy^{2-},a} = \frac{[H^+]\cdot[Cy^{3-}]}{[HCy^{2-}]} = 3 \times 10^{-14}$
(S4)	$H_2ClCy \rightleftharpoons H^+ + HClCy^-$	$K_{H_2ClCy,a} = \frac{[H^+]\cdot[HClCy^-]}{[H_2ClCy]} = 4.7 \times 10^{-6}$
(S5)	$HClCy^- \rightleftharpoons H^+ + ClCy^{2-}$	$K_{HClCy^-,a} = \frac{[H^+]\cdot[ClCy^{2-}]}{[HClCy^-]} = 7.6 \times 10^{-11}$
(S6)	$HCl_2Cy \rightleftharpoons H^+ + Cl_2Cy^-$	$K_{HCl_2Cy,a} = \frac{[H^+]\cdot[Cl_2Cy^-]}{[HCl_2Cy]} = 1.8 \times 10^{-4}$
(S7)	$H_2ClCy + H_2O \rightleftharpoons HOCl + H_3Cy$	$K_{H_2ClCy,h} = \frac{[HOCl]\cdot[H_3Cy]}{[H_2ClCy]} = 9 \times 10^{-5}$
(S8)	$HCl_2Cy + H_2O \rightleftharpoons HOCl + H_2ClCy$	$K_{HCl_2Cy,h} = \frac{[HOCl]\cdot[H_2ClCy]}{[HCl_2Cy]} = 1.2 \times 10^{-3}$
(S9)	$Cl_3Cy + H_2O \rightleftharpoons HOCl + HCl_2Cy$	$K_{Cl_3Cy,h} = \frac{[HOCl]\cdot[HCl_2Cy]}{[Cl_3Cy]} = 2 \times 10^{-2}$
(S10)	$HOCl \rightleftharpoons H^+ + OCl^-$	$K_{HOCl} = \frac{[H^+]\cdot[OCl^-]}{[HOCl]} = 2.88 \times 10^{-8}$

In addition to the ten equations shown in Table S1, there are two other equations: a mass balance equation for cyanurate species and a mass balance equation for free chlorine (FC). Equation (S11) below is the mass balance equation for cyanurate species:

$$Cy_{total} = [H_3Cy] + [H_2Cy^-] + [HCy^{2-}] + [Cy^{3-}] + [H_2ClCy] + [HClCy^-] + [ClCy^{2-}] + [HCl_2Cy] + [Cl_2Cy^-] + [Cl_3Cy] \quad \text{(S11)}$$

In Equation (S11), Cy_{total} is the total cyanurate concentration, as would be measured by a standard, turbidity based cyanuric acid test kit. Equation (S12) below is the FC mass balance equation:

$$FC_{total} = [HOCl] + [OCl^-] + [H_2ClCy] + [HClCy^-] + [ClCy^{2-}] + 2 \cdot \{[HCl_2Cy] + [Cl_2Cy^-]\} + 3 \cdot [Cl_3Cy] \quad \text{(S12)}$$

Note that FC_{total} corresponds to the measured "free" chlorine concentration and includes chlorinated isocyanurate species in addition to the free chlorine species hypochlorous acid, hypochlorite anion, and the generally insignificant Cl_2.

These twelve equations make it possible to calculate the concentrations of all twelve relevant species: the ten cyanurate species indicated in Equation (S11) plus the concentration of hypochlorous acid and hypochlorite—provided that the pH, total cyanurate concentration, and measured FC concentration are known.

To do so, Equations (S1) through (S9) in Table S1 were rearranged to provide ratios of the concentrations of each of the ten possible isocyanurate forms to the reference value $[H_3Cy]$. The resulting equations are shown in Table S2.

Table S2. Concentration ratios of the various isocyanurate species relative to H_3Cy.

#	Ref. #s [a]	Equation
(S13)	1	$\frac{[H_2Cy^-]}{[H_3Cy]} = \frac{K_{H_3Cy,a}}{[H^+]}$
(S14)	1, 2	$\frac{[HCy^{2-}]}{[H_3Cy]} = \frac{K_{H_2Cy^-,a}}{[H^+]} \cdot \frac{[H_2Cy^-]}{[H_3Cy]} = \frac{K_{H_3Cy,a} \cdot K_{H_2Cy^-,a}}{[H^+]^2}$
(S15)	1, 2, 3	$\frac{[Cy^{3-}]}{[H_3Cy]} = \frac{K_{HCy^{2-},a}}{[H^+]} \cdot \frac{[HCy^{2-}]}{[H_3Cy]} = \frac{K_{H_3Cy,a} \cdot K_{H_2Cy^-,a} \cdot K_{HCy^{2-},a}}{[H^+]^3}$
(S16)	7	$\frac{[H_2ClCy]}{[H_3Cy]} = \frac{[HOCl]}{K_{H_2ClCy,h}}$
(S17)	4, 7	$\frac{[HClCy^-]}{[H_3Cy]} = \frac{K_{H_2ClCy,a}}{[H^+]} \cdot \frac{[H_2ClCy]}{[H_3Cy]} = \frac{K_{H_2ClCy,a}}{K_{H_2ClCy,h}} \cdot \frac{[HOCl]}{[H^+]}$
(S18)	4, 5, 7	$\frac{[ClCy^{2-}]}{[H_3Cy]} = \frac{K_{HClCy^-,a}}{[H^+]} \cdot \frac{[HClCy^-]}{[H_3Cy]} = \frac{K_{H_2ClCy,a} \cdot K_{HClCy^-,a}}{K_{H_2ClCy,h}} \cdot \frac{[HOCl]}{[H^+]^2}$
(S19)	7, 8	$\frac{[HCl_2Cy]}{[H_3Cy]} = \frac{[HOCl]}{K_{HCl_2Cy,h}} \cdot \frac{[H_2ClCy]}{[H_3Cy]} = \frac{[HOCl]^2}{K_{H_2ClCy,h} \cdot K_{HCl_2Cy,h}}$
(S20)	6, 7, 8	$\frac{[Cl_2Cy^-]}{[H_3Cy]} = \frac{K_{HCl_2Cy,a}}{[H^+]} \cdot \frac{[HCl_2Cy]}{[H_3Cy]} = \frac{K_{HCl_2Cy,a}}{K_{H_2ClCy,h} \cdot K_{HCl_2Cy,h}} \cdot \frac{[HOCl]^2}{[H^+]}$
(S21)	7, 8, 9	$\frac{[Cl_3Cy]}{[H_3Cy]} = \frac{[HOCl]}{K_{Cl_3Cy,h}} \cdot \frac{[HCl_2Cy]}{[H_3Cy]} = \frac{[HOCl]^3}{K_{H_2ClCy,h} \cdot K_{HCl_2Cy,h} \cdot K_{Cl_3Cy,h}}$

[a] Indicates the equations from Table S1 used to develop the equation on the given row.

By adding up the concentration ratios of each of the ten possible isocyanurate forms (indicated in Equation (S11)) to the common, fully protonated form, H_3Cy, one can get an expression for the ratio of the total or measurable cyanuric acid concentration to the concentration of H_3Cy shown in Equation (S22) below:

$$\frac{Cy_{total}}{[H_3Cy]} = \frac{[H_3Cy]}{[H_3Cy]} + \frac{[H_2Cy^-]}{[H_3Cy]} + \frac{[HCy^{2-}]}{[H_3Cy]} + \frac{[Cy^{3-}]}{[H_3Cy]} + \frac{[H_2ClCy]}{[H_3Cy]} + \frac{[HClCy^-]}{[H_3Cy]} + \frac{[ClCy^{2-}]}{[H_3Cy]} + \frac{[HCl_2Cy]}{[H_3Cy]} + \frac{[Cl_2Cy^-]}{[H_3Cy]} + \frac{[Cl_3Cy]}{[H_3Cy]} \quad \text{(S22)}$$

The concentration $[H_3Cy]$ is equal to the total cyanurate concentration divided by the above ratio. Substituting the values from the right sides of Equations (S13) to (S21) in Table S2 into the denominator of the resulting expression gives Equation (S23), in which $[H_3Cy]$ is calculated solely from the total (or measurable) cyanuric acid concentration, the pH, and the hypochlorous acid concentration:

$$[H_3Cy] = Cy_{total} / \left(1 + \frac{K_{H_3Cy,a}}{[H^+]} \cdot \left(1 + \frac{K_{H_2Cy^-,a}}{[H^+]} \cdot \left(1 + \frac{K_{HCy^{2-},a}}{[H^+]} \right) \right) + \frac{[HOCl]}{K_{H_2ClCy,h}} \cdot \left(1 + \frac{K_{H_2ClCy,a}}{[H^+]} \cdot \left(1 + \frac{K_{HClCy^-,a}}{[H^+]} \right) + \frac{[HOCl]}{K_{HCl_2Cy,h}} \cdot \left(1 + \frac{K_{HCl_2Cy,a}}{[H^+]} + \frac{[HOCl]}{K_{Cl_3Cy,h}} \right) \right) \right) \quad \text{(S23)}$$

For purposes of future manipulation, it is convenient to represent the denominator of Equation (S23) as "D", so that the equation can be briefly expressed as $[H_3Cy] = Cy_{total}/D$.

The free chlorine mass balance, Equation S12, can now be expressed in terms of [$HOCl$], the known quantities Cy_{total}, [H^+], and the various equilibrium constants by use of Equations (S10), (S16)–(S21), and (S23).

$$FC_{total} = [HOCl] \cdot \left(1 + \frac{K_{HOCl}}{[H^+]}\right) + \frac{Cy_{total}}{D} \cdot \left\{\frac{[HOCl]}{K_{H_2ClCy,h}} \cdot \left(1 + \frac{K_{H_2ClCy,a}}{[H^+]} \cdot \left(1 + \frac{K_{HClCy^-,a}}{[H^+]}\right) + \frac{2 \cdot [HOCl]}{K_{HCl_2Cy,h}} \cdot \left(1 + \frac{K_{HCl_2Cy,a}}{[H^+]} + \frac{3 \cdot [HOCl]}{2 \cdot K_{Cl_3Cy,h}}\right)\right)\right\} \quad \text{(S24)}$$

Abbreviating the portion of Equation (S24) in brackets, with the letter B, the equation simplifies to the following:

$$FC_{total} = [HOCl] \cdot \left(1 + \frac{K_{HOCl}}{[H^+]}\right) + \frac{Cy_{total}}{D} \cdot B \quad \text{(S25)}$$

Both B and D in Equation (S25) are functions of [$HOCl$], so the derivative of free chlorine with respect to [$HOCl$] involves derivatives of these functions:

$$\frac{dFC_{total}}{d[HOCl]} = \left(1 + \frac{K_{HOCl}}{[H^+]}\right) + Cy_{total} \cdot \frac{D \cdot \frac{dB}{d[HOCl]} - B \cdot \frac{dD}{d[HOCl]}}{D^2} \quad \text{(S26)}$$

The derivative of D is as follows:

$$\frac{dD}{d[HOCl]} = \frac{1}{K_{H_2ClCy,h}} \cdot \left(1 + \frac{K_{H_2ClCy,a}}{[H^+]} \cdot \left(1 + \frac{K_{HClCy^-,a}}{[H^+]}\right) + \frac{2 \cdot [HOCl]}{K_{HCl_2Cy,h}} \cdot \left(1 + \frac{K_{HCl_2Cy,a}}{[H^+]} + \frac{3 \cdot [HOCl]}{2 \cdot K_{Cl_3Cy,h}}\right)\right) \quad \text{(S27)}$$

The derivative of B is as follows:

$$\frac{dB}{d[HOCl]} = \frac{1}{K_{H_2ClCy,h}} \cdot \left(1 + \frac{K_{H_2ClCy,a}}{[H^+]} \cdot \left(1 + \frac{K_{HClCy^-,a}}{[H^+]}\right) + \frac{4 \cdot [HOCl]}{K_{HCl_2Cy,h}} \cdot \left(1 + \frac{K_{HCl_2Cy,a}}{[H^+]} + \frac{9 \cdot [HOCl]}{4 \cdot K_{Cl_3Cy,h}}\right)\right) \quad \text{(S28)}$$

Plugging the values for B, D, $dB/d[HOCl]$, and $dD/d[HOCl]$ into Equation (S26) gives an expression for the derivative of free chlorine with respect to hypochlorous acid concentration:

$$\begin{aligned}\frac{dFC_{total}}{d[HOCl]} = \left(1 + \frac{K_{HOCl}}{[H^+]}\right) + Cy_{total} \cdot \Bigg(\Bigg(\left(1 + \frac{K_{H_3Cy,a}}{[H^+]} \cdot \left(1 + \frac{K_{H_2Cy^-,a}}{[H^+]} \cdot \left(1 + \frac{K_{HCy^{2-},a}}{[H^+]}\right)\right) + \frac{[HOCl]}{K_{H_2ClCy,h}} \cdot \\ \left(1 + \frac{K_{H_2ClCy,a}}{[H^+]} \cdot \left(1 + \frac{K_{HClCy^-,a}}{[H^+]}\right) + \frac{[HOCl]}{K_{HCl_2Cy,h}} \cdot \left(1 + \frac{K_{HCl_2Cy,a}}{[H^+]} + \frac{[HOCl]}{K_{Cl_3Cy,h}}\right)\right)\right) \cdot \frac{1}{K_{H_2ClCy,h}} \cdot \\ \left(1 + \frac{K_{H_2ClCy,a}}{[H^+]} \cdot \left(1 + \frac{K_{HClCy^-,a}}{[H^+]}\right) + \frac{4 \cdot [HOCl]}{K_{HCl_2Cy,h}} \cdot \left(1 + \frac{K_{HCl_2Cy,a}}{[H^+]} + \frac{9 \cdot [HOCl]}{4 \cdot K_{Cl_3Cy,h}}\right)\right) - \left(\frac{[HOCl]}{K_{H_2ClCy,h}} \cdot \right. \\ \left(1 + \frac{K_{H_2ClCy,a}}{[H^+]} \cdot \left(1 + \frac{K_{HClCy^-,a}}{[H^+]}\right) + \frac{2 \cdot [HOCl]}{K_{HCl_2Cy,h}} \cdot \left(1 + \frac{K_{HCl_2Cy,a}}{[H^+]} + \frac{3 \cdot [HOCl]}{2 \cdot K_{Cl_3Cy,h}}\right)\right)\Bigg) \cdot \Bigg(\frac{1}{K_{H_2ClCy,h}} \cdot \\ \left(1 + \frac{K_{H_2ClCy,a}}{[H^+]} \cdot \left(1 + \frac{K_{HClCy^-,a}}{[H^+]}\right) + \frac{2 \cdot [HOCl]}{K_{HCl_2Cy,h}} \cdot \left(1 + \frac{K_{HCl_2Cy,a}}{[H^+]} + \frac{3 \cdot [HOCl]}{2 \cdot K_{Cl_3Cy,h}}\right)\right)\Bigg)\Bigg) /\end{aligned} \quad \text{(S29)}$$

$$\left(1+\frac{K_{H_3Cy,a}}{[H^+]}\cdot\left(1+\frac{K_{H_2Cy^-,a}}{[H^+]}\cdot\left(1+\frac{K_{HCy^{2-},a}}{[H^+]}\right)\right)+\frac{[HOCl]}{K_{H_2ClCy,h}}\cdot\left(1+\frac{K_{H_2ClCy,a}}{[H^+]}\cdot\left(1+\frac{K_{HClCy^-,a}}{[H^+]}\right)+\frac{[HOCl]}{K_{HCl_2Cy,h}}\cdot\left(1+\frac{K_{HCl_2Cy,a}}{[H^+]}+\frac{[HOCl]}{K_{Cl_3Cy,h}}\right)\right)\right)^2$$

Using the above equations, the procedure used to calculate the concentration of hypochlorous acid (as well as the concentrations of the various isocyanurate species and of hypochlorite anion) was as follows:

1. The free chlorine concentration was converted from milligrams per liter (or parts per million) to molarity by dividing the mg/L concentration by 70,906 milligrams of chlorine per mole.
2. Similarly, the pH was converted to hydrogen ion molar concentration, or to be more precise, hydrogen ion activity, using the standard conversion: $[H^+] \cong a_{H^+} = 10^{-pH}$.
3. The iterative calculation was started with an arbitrary initial assumed concentration for hypochlorous acid. (For this work. the starting value was 0 mg/L, though other first iteration hypochlorous acid concentrations could be used and the same final result is obtained after several iterations of the following steps.)
4. By plugging the hydrogen ion activity (from step 2) and the hypochlorous acid concentration (initially from step 3) into Equations (S13)–(S21) in Table S2, the concentration ratios of each of the ten isocyanurate species to [H_3Cy] was calculated, with [H_3Cy]/[H_3Cy], of course, being 1, regardless of the hydrogen ion or hypochlorous acid concentrations.
5. The ratios of all ten cyanurate species to the common form (H_3Cy) were summed to determine the ratio of the total cyanurate concentration to H_3Cy in Equation (S22).
6. The total (reported, measured) cyanuric acid concentration was divided by the ratio indicated in step 5 to calculate the H_3Cy concentration for the current iteration in Equation (S23).
7. Each of the ratios calculated in step 4 was multiplied by the [H_3Cy] concentration calculated in step 6 to get the first estimate of the molar concentrations of each of the ten cyanurate forms.
8. A resulting FC concentration was calculated for the current iteration using Equation (S24).
9. For the next iteration, the assumed *HOCl* concentration was revised using the Newton–Raphson method, in this case, based on the error in the free chlorine sum calculated in step 8:

$$[HOCl]_{i+1} = [HOCl]_i + \frac{FC_{meas}-FC_{calc}}{\frac{dFC}{d[HOCl]}}, \quad \text{(S30)}$$

where $[HOCl]_i$ represents the hypochlorous acid concentration used for the iteration just completed and $[HOCl]_{i+1}$ is the concentration for the next iteration; FC_{meas} is the reported, measured free chlorine; FC_{calc} is the summed chlorine from step 8, i.e., FC_{total}; and the differential $dFC/d[HOCl]$ is the first derivative of FC_{calc} as a function of [*HOCl*], using Equation (S29). With a new, closer, estimate of the *HOCl* concentration, steps 3 through 9 were repeated. Iterations continued until convergence was achieved, namely $FC_{calc} = FC_{meas}$. Convergence was generally achieved in a few iterations.

Three authors of this paper independently derived similar methods to those described above. Another derivation is given in the supplemental PDF file "Computing HOCl.pdf", which defines intermediate calculations used in the model workbook. In addition, during the writing of this paper, Wahman [2] presented chlorinated cyanurate equations (in Wahman's Figure 5) and an open-form solution equivalent to those in this paper.

S3. Ionic Strength Correction

The equilibrium constant for hypochlorous acid dissociation was adjusted to account for the impact of ionic strength on hypochlorite ion activity. The 10^{-pH} calculation gives hydrogen ion activity directly rather than hydrogen ion concentration, so no ionic strength adjustment is needed for it. Moreover, neutral molecules, such as hypochlorous acid, do not require a significant ionic strength adjustment in conversion to activity except at a very high ionic strength. Consequently, only the hypochlorite ion concentration requires an adjustment based on ionic strength.

The activity coefficient for hypochlorite was calculated using the Davies equation:

$$Log(\gamma^-) = -A\,Z^2\,[I^{0.5}/(1 + I^{0.5}) - 0.3\,I], \quad \text{(S31)}$$

where γ^- is the anion (hypochlorite in this case) activity coefficient, A is a constant (approximately 0.51), Z is ion charge (−1 in this case), and I is the ionic strength (molarity) of the solution. The constant A depends on the dielectric constant, temperature, and solution density. For water, the value of A is as follows:

$$A = 1.8246 \times 10^6 \times D^{0.5} \times (\epsilon T)^{-1.5}, \quad \text{(S32)}$$

where D, the density of the water (g/mL), can be rounded to 1 without significant impact on the accuracy of the activity coefficient; T is temperature (K); and ϵ is the dielectric constant of water as a function of temperature [3]:

$$\epsilon = 87.740 - 0.40008T + (9.398 \times 10^{-4})T^2 - (1.410 \times 10^{-6})T^3. \quad \text{(S33)}$$

Such ionic strength adjustments were not needed for the hydrolysis constants of the chlorinated isocyanurates, as there was no net change in number of ions or ion charge in these reactions. However, for the acid hydrolysis reactions (Reactions (S1)–(S6) and the corresponding equations in Table S1), the ionic strength impact on the relevant cyanurate anions was taken into account. As indicated above, no activity coefficients were needed for the hydrogen ions, since pH relates to hydrogen ion activity rather than concentration.

To simplify the calculation of hypochlorous acid concentration, especially in the presence of cyanuric acid, which greatly complicates the calculations, the activity coefficients were used to adjust the equilibrium constants to the relevant ionic strength rather than separately converting all the individual anion concentrations to corresponding activities.

Since O'Brien's work was performed in aqueous solutions of 0.02 M ionic strength, and the equilibrium constants were calculated based on concentration and not corrected for activity [4] (esp. p. 39 and Table R-XV, p. 87), it was first necessary to correct the acid ionization constants to 0 M ionic strength by adding the activity coefficient (which was approximately $0.51 \times [\,0.02^{0.5} / (1 + 0.02^{0.5}) - 0.3 \times 0.02\,] = 0.06$ times the relevant anion charge squared) to the ionization constants reported by O'Brien.

Once the equilibrium constants for Equations (S1)–(S6) were converted to true, activity-based equilibrium constants, they could then be adjusted to other ionic strengths by using Equation (S31). In this case, it should be noted that, while the value Z is −1 in half the cases, for the equilibrium constants in Equations (S2) and (S5), $Z_{product}$ and $Z_{reactant}$ are −2 and −1 respectively and, in Equation (S3), are −3 and −2; so for instance, in view of Equation (S31), the relevant activity coefficient adjustment for Equation (S3) is $3^2 - 2^2 = 5$ times the pK correction relative to Equation (S1) which

involves an uncharged molecule and a monoanion, apart from the hydrogen ion which requires no correction.

It may be noted that ionic strength corrections were generally not large. When typical cyanuric acid concentrations are involved, the error contribution from ionic strength would typically be a <4% relative change in hypochlorous acid concentration in a Total Dissolved Solids (TDS) range of 500 to 3000 mg/L at the lower pH of 7.0, where the effect is greater.

Ionic strength can be estimated from TDS, using Langelier's approximation [5], which has gained wide acceptance [6]:

$$I = 2.5 \times 10^{-5} \times TDS. \quad \text{(S34)}$$

In the current work, this relationship was assumed for TDS ≤ 500 mg/L. For TDS above 500 mg/L, it was assumed that the primary contributor to TDS above 500 mg/L is sodium chloride from the buildup of consumed chlorine or intentionally added for saltwater chlorine generators, for which the ionic strength contribution would be 1.7×10^{-5} times the TDS. This is based on the formula weight for sodium chloride (58,443 mg/mole) and the Lewis and Randall formula for ionic strength [7]:

$$I = \frac{1}{2}\sum_i c_i \cdot z_i^2, \quad \text{(S35)}$$

where c is concentration (molarity) and z is ionic charge. In the case of sodium chloride, c is 1 M for each 58,443 mg/L TDS. Since the charge for both the sodium and chloride ions is 1 each, this whole equation reduces to the following:

$$I = \frac{1}{2}(1^2 + 1^2) \times TDS/58{,}443 = 1.71 \times 10^{-5} \times TDS. \quad \text{(S36)}$$

Thus, conversion from TDS to ionic strength is as follows:

For TDS ≤ 500 mg/L: $I = 2.5 \times 10^{-5} \times TDS$
For TDS > 500 mg/L: $I = 2.5 \times 10^{-5} \times 500 + 1.7 \times 10^{-5} \times (TDS - 500)$ (S37)

S4. Temperature Compensation

Morris has provided data on the acid deprotonation constant of HOCl as a function of temperature over the range 0 to 35 °C [8] and the following equation (Equation (13) in Morris) was used in the model:

$$pK_{HOCl} = \frac{3000.00}{T} - 10.0686 + 0.0253\mathrm{T}. \quad \text{(S38)}$$

Adding the log of the hypochlorite activity coefficient, Equations (S31)–(S38) give a pK_{HOCl} adjusted for both temperature and ionic strength.

S4.1. Wojtowicz and Solastiouk

The only temperature corrections employed for cyanurate-related equilibrium constants were for the constants $K_{H3Cy,a}$, $K_{Cl2Cy^-,h}$, and $K_{HClCy^-,h}$ and constants derived from these constants, as in Equations (S41) and (S42) below. This is because, at the usual low chlorine to cyanuric acid ratios and usual pH in swimming pools, the dominant cyanurate is H_2Cy^- and the dominant chlorinated

cyanurate is $HClCy^-$. The concentrations of these dominant species are influenced by these constants (when using the model in the supplemental PowerPoint presentation file "Computing HOCl revised.pptx"). Wojtowicz [9] provided temperature corrections for the chlorinated constants using measurements from Pinsky and Hu [10] at temperatures of 15.5, 25, and 30 °C. For the current work, O'Brien's pK values at 25 °C were used but with temperature corrections for other temperatures based on the hydrolysis enthalpies from Wojtowicz:

$$K_{Cl_2Cy^-,h} = \frac{[HOCl]\cdot[HClCy^-]}{[Cl_2Cy^-]} = 3.09 \times 10^{-5} \times e^{11{,}078\left(\frac{1}{298}-\frac{1}{T}\right)} = 4.23 \times 10^{11} \times e^{-11{,}078/T} \quad \text{(S39)}$$

$$K_{HClCy^-,h} = \frac{[HOCl]\cdot[H_2Cy^-]}{[HClCy^-]} = 2.40 \times 10^{-6} \times e^{11{,}912\left(\frac{1}{298}-\frac{1}{T}\right)} = 5.39 \times 10^{11} \times e^{-11{,}912/T} \quad \text{(S40)}$$

In the above corrections, 3.09 × 10^{-5} M and 2.40 × 10^{-6} M are the values of the indicated equilibrium constants at 25 °C reported by O'Brien and 11,078 K and 11,912 K are the ΔH/R values (slope of a plot of Ln(1/K) versus 1/T) reported by Wojtowicz.

The temperature-adjusted values of $K_{HClCy^-,h}$ and $K_{Cl2Cy^-,h}$ could also be used to provide temperature corrected values for $K_{H2ClCy,h}$ and $K_{HCl2Cy,h}$ in the model detailed in Supplementary Material S1:

$$K_{H_2ClCy,h} = K_{HClCy^-,h} \times K_{H_2ClCy,a}/K_{H_3Cy,a} \quad \text{(S41)}$$

$$K_{HCl_2Cy,h} = K_{Cl_2Cy^-,h} \times K_{HCl_2Cy,a}/K_{H_2ClCy,a} \quad \text{(S42)}$$

The temperature dependence on $K_{H3Cy,a}$ was taken from Solastiouk [11] based on the following equation adjusted with the 0.085494 constant to match the equilibrium constant at 25 °C reported by O'Brien:

$$K_{H_3Cy,a} = 10^{-\left(0.085494+31.08-0.154T+2.441\times10^{-4}T^2\right)} \quad \text{(S43)}$$

S4.2. Wahman

During the writing of this paper, improved temperature dependence and equilibrium constants were determined by Wahman [12] for $K_{H3Cy,a}$ and by Wahman and Alexander [13] for $K_{HClCy^-,h}$ and $K_{Cl2Cy^-,h}$. These are incorporated as an option in the model workbook based on the following equations (the pK_6, pK_{7a}, and pK_{9a} are the equivalent constants used in the Wahman papers):

$$pK_{H_3Cy,a} = pK_6 = \frac{1743}{T_K} + 1.12 \quad \text{(S44)}$$

$$pK_{Cl_2Cy,h} = pK_{7a} = \frac{2028}{T_K} - 2.15 \quad \text{(S45)}$$

$$pK_{HClCy,h} = pK_{9a} = \frac{2229}{T_K} - 1.65 \quad \text{(S46)}$$

S5. Disinfection Kinetics Sources

Studies of the effect of CYA on disinfection rates have been conducted by a number of researchers over several decades. Table S3 provides a summary of the effects of CYA on microbial inactivation kinetics for several waterborne microbes.

Table S3. Summary of literature reports of the effects of CYA on microbial inactivation by chlorine.

Organism	Reference
Bacteria	
Streptococcus faecalis, Staphylococcus aureus	[14]
Streptococcus faecalis, Staphylococcus aureus	[15]
Streptococcus faecalis	[16]
Pseudomonas aeruginosa	[17]
Pseudomonas aeruginosa, Streptococcus faecalis, and *Staphylococcus aureus*	[18]
Escherichia coli, Streptococcus faecalis, Staphylococcus aureus	[19]
Staphylococcus aureus, Streptococcus faecalis, Pseudomonas aeruginosa, Escherichia coli, Proteus mirabilis, Candida albicans	[20]
Escherichia coli	[21]
Amoeba	
Naegleria gruberi	[22]
Protozoa	
Cryptosporidium parvum	[23]
Cryptosporidium parvum	[24]
Algae	
Pleurochloris pyrenoidosa, Phormidium minnesotense, Oocystis sp.	[25]
Virus	
Poliovirus	[26]
Poliovirus	[27]
Polio 1 and 2; Coxsackie A24, B3, B4, and B5; Echo 6, 7, and 11; Entero 70; Adeno 3 and 7	[28]
Poliovirus 1, Coxsackievirus A24, Enterovirus 70, Adenovirus type 3	[29]
Poliovirus 1	[30]

In addition to these studies, various reports on the effects of cyanuric acid have also been published from field studies. Table S4 summarizes pertinent aspects of these studies.

Table S4. Summary of the results of field experiments to examine the effects of CYA on microbial inactivation of waterborne microbes by free chlorine

Number of pools	Chemical information provided	Organisms measured	References
193 pools	FC, pH, CYA	Coliforms, fecal streptococci, total staphylococci, *Pseudomonas aeruginosa*, standard plate count	[31]
42 spas	FC, pH, CYA (only if present or not)	*Pseudomonas aeruginosa*, amoeba (*Naegleria australiensis*, *Naegleria* sp., *Acanthomoeba* spp, *Willaertia magna)*	[32]
12 pools	FC, pH, sanitizer type	Total counts, Staphylococci, enterococci, *Streptococcus salivarius*, coliform bacteria, *Pseudomonas aeruginosa*	[33]
153 pools (15 in 1960, 138 in 1963)	FC, pH, CYA	Total plate count, *Escherichia coli*	[34]
3750 pools	Sanitizer type	Staphylococci, *Pseudomonas aeruginosa*, coliforms	[35]
6 pools	sanitizer type, FC, pH, CYA	Total plate counts, coliforms	[30]

The literature generally shows that CYA increases the kill times for FC. In contrast, the literature indicates that CYA has little effect on the efficacy of combined chlorine, such as monochloramine, since amines bind available chlorine more strongly than CYA [16,17]. CYA also has no effect on the efficacy of available bromine, since CYA does not bind bromine strongly enough. It is well-known that CYA does not stabilize available bromine against sunlight degradation in a swimming pool [36,37].

S6. Average Shedding Rate Formula

The time-dependent shedding rate shown in Figure 1 in Elmir [38] was seen to have a rough exponential decay over time:

$$Rate = InitialRate \times e^{-kt}. \quad \text{(S47)}$$

The steady-state solution to the advective-diffusion model in Equation (7) and Equation (8) in the main paper assumes a constant rate of introduction of pathogen ($\dot{m}$). Therefore, it was necessary to calculate an average pathogen introduction rate over the time that the shedding bather is in the water. It was assumed that this time is the same as the exposure time for ingesting bathers. To get the average rate over this time, the rate was integrated to get the cumulative amount:

$$Cumulative = \left(\frac{InitialRate}{k}\right)(1 - e^{-kt}). \quad \text{(S48)}$$

Dividing by the time interval "t" gives the average rate given as Equation (3) in the main paper:

$$AverageRate = InitialRate\left(\frac{1-e^{-kt}}{kt}\right). \quad \text{(S49)}$$

The Elmir data was fit to the rate formula Equation (S47) to determine the "k" value of 0.0309 min^{-1} used in the model workbook. An alternative approach shown in the supplemental workbook "ElmirFit.xlsx" computed cumulative amounts and was fit to the cumulative formula Equation (S48) to determine the "k" value of 0.0464, which is a faster decay so is less conservative and was not used in the model.

A more realistic model would be a combination of release of built-up fecal material (perhaps with exponential or other modeled decay) combined with a fixed low-level leakage, but there is insufficient data to create a better model at this time. Measurements of fecal indicator bacteria are influenced by the more than order-of-magnitude variation in concentration of bacteria among individuals (References [39,40] for *E. coli*). Future studies using indicator bacteria should measure its concentration in each individual's fecal matter in addition to the absolute amount released.

S7. Inactivation Constant α from U.S. EPA Ct Table

The Ct tables published by the U.S. EPA for *Giardia* [41] have a temperature dependence that has the Ct value cut in half, equivalent to a doubling of the inactivation rate, for every 10 °C increase in temperature. This is described in more detail in Section S8.

The Ct values at 5 °C were used to develop formulas for the inactivation constant at different chlorine concentration (rows of EPA table) and pH (columns of EPA table).

Because the inactivation rate was presumed to be based on the HOCl concentration and not on FC, an HOCl/FC factor was calculated for each pH. The inactivation constant was calculated from the Chick–Watson equation modified to account for die-off and assuming a dilution coefficient "n" of 1 and recognizing that the EPA table was for a 3-log_{10} reduction:

$$ln(N_t/N_0) = -\ln(10) \times 3 = -(\alpha C + d)t = -\alpha(Ct) - dt \quad \text{(S50)}$$

$$\alpha = \frac{\ln(10)\times 3 - d\cdot t}{(HOCl/FC)(Ct)} = \frac{\ln(10)\times 3}{(HOCl/FC)(Ct)} - \frac{d}{(HOCl/FC)C} \quad \text{(S51)}$$

The "Ct" was taken from the EPA table but adjusted to equivalent Ct based on the HOCl concentration rather than the free chlorine concentration. In the divisor for die-off, the concentration "C" was taken from the EPA table row chlorine concentration value, and this was also adjusted to the equivalent of HOCl. The result of applying Equation (S51) is to create a new table of inactivation constants.

To interpolate between the values in the table, a simple linear regression was performed for each column of the table (i.e., for each pH value). Interpolation between the columns (pH values) was done via a table of slopes and intercepts for each pH where simple linear interpolation was done to give intermediate slope and intercept values.

Interestingly, the inactivation constants are within a 20% range from pH 6.0 to 7.5 but increase significantly at higher pH, implying either that hypochlorite ion (OCl^-) has about 1/3rd the inactivation capability of hypochlorous acid (HOCl) or that there is some other pH enhancement to inactivation of *Giardia* by chlorine.

S8. Ct Temperature Adjustment

Ct values in the literature are not always measured at 25 °C and not always at a pH of 7.5, so for calculating a standardized inactivation constant at 25 °C and using HOCl, the Ct values for *E. coli* and *Cryptosporidium* were adjusted using the following equation, where it is assumed that there is a doubling of disinfection/inactivation rates or, equivalently, a halving of Ct value with every 10 °C temperature increase.

$$adjusted\ Ct = Ct\frac{2^{\frac{25-Temp}{10}}}{1+10^{(pH-7.474)}} \quad \text{(S52)}$$

The inactivation rate constant (α) was calculated using this adjusted Ct in Equation (5) in the main paper. This makes this constant based on HOCl and independent of pH for *E. coli* and *Cryptosporidium* (as noted in Section S7, *Giardia* inactivation rate constants were calculated from EPA tables and have an unexplained pH dependence particularly above pH 7.5). Temperature dependence in the model is then based on assuming a doubling of the inactivation rate constant with every 10 °C temperature increase.

S9. Secondary Disinfection and Filtration

The model workbook includes an option to specify secondary disinfection (or filtration) with a specified log-reduction per pass and a turnover time (the time for one pool volume of water to circulate through the system). As shown in Table S5, a filtration system with 1-log (90%) removal is nearly as effective as a secondary disinfection system with a 3-log (99.9%) reduction. This is due to the law of dilution as first specified by Gage and Bidwell [42], where the fraction of total pool volume that has gone through the circulation (and disinfection and filtration) system is $1 - e^{-T}$, where T is the number of turnovers (full pool water volumes). The following Table S5 shows the effect of different levels of log-reduction in a secondary disinfection or filtration system with a CYA/FC ratio of 45 and a 6-hour turnover.

Table S5. Probability of infection (CYA/FC = 45; 6-hour turnover)

	secondary disinfection or filtration log reduction (%)					
Pathogen/Per-Visit Risk [a]	0 (0%)	0.10 (20%)	0.30 (50%)	1 (90%)	2 (99%)	3 (99.9%)
Escherichia coli O157	8.3×10^{-6}	8.3×10^{-6}	8.3×10^{-6}	8.3×10^{-6}	8.3×10^{-6}	8.3×10^{-6}
Giardia	1.3×10^{-3}	1.1×10^{-3}	9.3×10^{-4}	7.8×10^{-4}	7.5×10^{-4}	7.5×10^{-4}
Cryptosporidium parvum	1.4×10^{-4}	3.0×10^{-5}	2.2×10^{-5}	1.9×10^{-5}	1.9×10^{-5}	1.9×10^{-5}
Pathogen/Annual Risk [b]	0 (0%)	0.10 (20%)	0.30 (50%)	1 (90%)	2 (99%)	3 (99.9%)
Escherichia coli O157	1.3×10^{-6}	1.3×10^{-6}	1.3×10^{-6}	1.3×10^{-6}	1.3×10^{-6}	1.3×10^{-6}
Giardia	7.1×10^{-2}	5.8×10^{-2}	4.6×10^{-2}	3.5×10^{-2}	3.4×10^{-2}	3.4×10^{-2}
Cryptosporidium parvum	9.0×10^{-3}	8.7×10^{-4}	3.7×10^{-4}	2.1×10^{-4}	2.0×10^{-4}	1.9×10^{-4}

[a] Risk with ingestor near shedder

[b] Risk averaged over varying distance from shedder to ingestor

Because *E. coli* is killed so quickly by chlorine, there is no effect of the secondary disinfection or filtration system on this pathogen. Likewise, there is only a modest reduction of probability of infection for *Giardia* since the rate of disinfection is significantly faster than the turnover time. However, for *Cryptosporidium*, there is a substantial reduction in risk even with a modest 0.1 log (20%) reduction since the disinfection rate is slower than the turnover time.

S10. Geometric Series Projection

The model workbook has a limited size for the number of bathers whose shedding is computed in an otherwise infinitely sized swimming pool. The calculation sums the effect of shedders in rings around a central ingestor. (The rings may be offset if one is closer to a particular bather.) To improve the accuracy of calculation, the relationship between the number of bathers in each ring and the

dilution and disinfection of pathogens was examined as one looks at the effects from more distant shedders.

The number of shedders in an annular ring of inner radius r and width dr around a central ingestor is described by Equation (S53). The ratio of shedders at radial position $r+dr$ to shedders at radial position r is described by Equation (S54):

$$Shedders = \frac{Shedders}{Area} \times 2\pi r \times dr \tag{S53}$$

$$\frac{Shedders\ at\ r+dr}{Shedders\ at\ r} = \frac{r+dr}{r} \tag{S54}$$

The solution to the spherical diffusion equation (see Reference [43]) is described by Equation (S55). The ratio of pathogen concentration at a radial position of $r+dr$ to the concentration at position r is described by Equation (S56):

$$P = \frac{\dot{m}}{4\pi Dr} e^{-\sqrt{\frac{\alpha C}{D}}r} \tag{S55}$$

$$\frac{P_1\ at\ r+dr}{P_1\ at\ r} = \frac{r}{r+dr} e^{-\sqrt{\frac{\alpha C}{D}}(r+dr-r)} = \frac{r}{r+dr} e^{-\sqrt{\frac{\alpha C}{D}}dr} \tag{S56}$$

Multiplying Equations (S54) and (S56) together indicates that terms dependent on radius cancel, and we have the pathogen concentration ratio dependent on the differential width of an annular ring (dr):

$$\frac{P_{all}\ at\ r+dr}{P_{all}\ at\ r} = e^{-\sqrt{\frac{\alpha C}{D}}dr} \tag{S57}$$

Because this differential width is constant, this implies that the ratio of pathogen contribution from a ring of shedders from successively more distant rings is constant. This is the definition of a geometric series whereby it has a constant ratio between successive terms. While the model workbook uses squares of bathers and not circular rings, the use of a geometric series projection, nevertheless, produces a realistic result. The ratio converges and becomes increasingly accurate with more distant squares of bathers on the grid.

The model workbook does an accurate sum for the 21 × 21 grid of bathers explicitly defined but then adds in the projected sum for the rest of the terms of the geometric series using the ratio of the sums of two outermost squares of the grid and the sum from the outermost square that is the starting term of the series:

$$ProjectedSum = \frac{RingSum_N}{1-\frac{RingSum_N}{RingSum_{N-1}}} \tag{S58}$$

$$Total = RingSum_1 + \cdots + RingSum_{N-1} + ProjectedSum \tag{S59}$$

S11. Pathogen Prevalence

The prevalence of each pathogen in the population (i.e., the percentage of infected individuals at any one point in time) was determined in the manner described below for each pathogen.

S11.1. E. coli (STEC)

Shiga toxin-producing *E. coli* (STEC) is tracked via active surveillance data. Table 2 in Majowicz et al. [44] for WHO subregion AMR A (U.S., Canada, and Cuba) gives a mean incidence of 93.5 per 100,000 person-years. This rate of 93.5/100,000 = 0.0935% was used in the model workbook.

A similar estimated incidence is given in Scallan et al. [45], where the total STEC (O157 and non-O157) is (3,704 × 26.1) + (1,579 × 106.8) = 265,312 out of a 2006 U.S. population of 299,000,000 for a rate of 0.0887%.

Because symptoms typically last for 1–4 weeks, these annual incidence rates overestimate the likely incidence at any single point in time but were used in the model as a conservative estimate. The length of shedding is not known, so the incidence value was not adjusted to prevalence.

S11.2. Giardia

The prevalence of parasites in fecal material (formed stools) from chlorinated swimming pools was determined in CDC's Morbidity and Mortality Weekly Report (MMWR) [46], where 4.4% of 293 formed stools had *Giardia* detected. This rate was used in the model workbook. This may be an overestimate if those infected with *Giardia* were more likely to defecate in the pool and may be biased more towards children if they are more likely to defecate in the pool.

Hellard et al. [47] reported an incidence rate of 1.6% for *Giardia* in 1093 asymptomatic individuals in Melbourne, Australia. Those aged ≤10 years had a higher incidence of 2.7% compared to those older with an incidence of 0.9%.

Furness et al. [48] states that "The prevalence of *Giardia* in stool specimens submitted for examination ranges from 2% to 5% in industrialized countries and from 20% to 30% in developing countries, and it can be as high as 35% among children attending day care centers in the United States in a nonoutbreak setting."

The incidence rate given in Scallan et al. [45] is 20,305 × 1.3 × 46.3 = 1,222,158 out of a 2006 U.S. population of 299,000,000 for a rate of 0.41%.

S11.3. Cryptosporidium

Hellard [47] reported an incidence rate of 0.4% for *Cryptosporidium* in 1093 asymptomatic individuals in Melbourne, Australia. Those aged ≤10 years had a higher incidence of 0.9% compared to those older with an incidence of 0%. The 0.4% rate was used in the model workbook.

The prevalence of parasites in fecal material (formed stools) from chlorinated swimming pools was determined in CDC's MMWR [46], where 0% of 293 formed stools had *Cryptosporidium* detected, implying a rate of <0.3%.

The incidence rate given in Scallen et al. [45] is 7594 × 98.6 = 748,768 out of a 2006 U.S. population of 299,000,000 for a rate of 0.25%.

S12. Mirror Image Sources

The swimming pool floor and the water surface exposed to air are boundaries where the flux must be zero. The linearity of the advective-diffusion equation makes it possible to achieve the boundary condition by adding additional sources at mirror image positions across each boundary. These mirror image sources effectively simulate the reflection at each boundary and result in a higher concentration near a boundary. If there were only a single reflection, the concentration at the boundary would be doubled.

The mirror image sources also add flux to the more distant boundary, thereby requiring higher order mirror image sources to cancel their effect and to maintain the zero flux condition at each

boundary. There is an infinite number of mirror image sources needed to produce the zero-flux condition, but the model workbook uses a limit of 100 such source pairs and the calculations are done using macros to sum the calculation result from each image plane. Figure S3 illustrates the placement of the mirror image sources and the relevant distances where "L" is the distance between the two boundaries (floor and water surface) and "S" is the distance from one boundary (e.g., the floor) to the original shedding source.

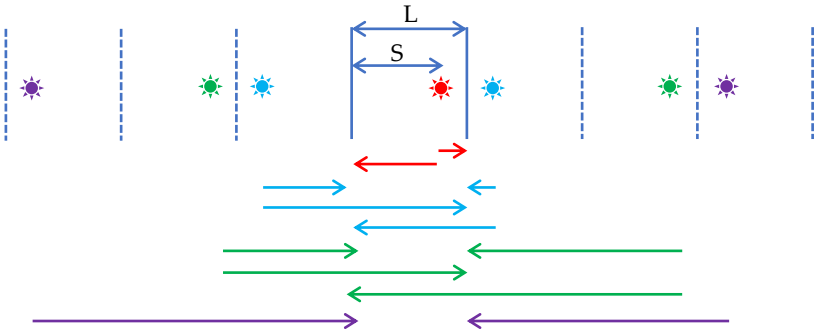

Figure S3. Placement of mirror image sources. Red is original shedder source. S is distance of source from left boundary. L is distance between boundaries. Blue shows first-order mirror image sources, green shows second-order sources, and purple shows third-order sources.

Table S6 shows the positions of the mirror image sources relative to the original source. The model workbook adjusts the "z" vertical distance of the ingestor to simulate the shift in the plane of shedding sources for their mirror image positions. The final entry in the table shows the classic mirror image position when halfway between boundaries (S=L/2), but in general, the odd and even formulas must be used instead.

Table S6. Mirror Image Positions

Order	Left Image Position	Right Image Position
0	0	0
1	−2S	+2(L−S)
2	−2L	+2L
3	−2S−2L	+2(L−S)+2L
Odd	−2S−(Order−1)*L	+2(L−S)+(Order−1)*L
Even	−Order*L	+Order*L
S=D/2	−Order*L	+Order*L

S13. Well-Mixed Model and Transition Thresholds

S13.1. Well-Mixed Model

In the main paper, Equation (9) was derived by assuming that the pathogen introduction rate is constant, that the pool water is well-mixed (i.e., no variation in the pathogen concentration with position), that a steady state is reached in which the removal rate (disinfection + die-off rate) becomes equal to the pathogen shedding rate, and that this steady state is reached immediately. The following equation shows how the die-off rate can be added to the Chick–Watson equation to obtain the rate of removal for both disinfection and die-off:

$$\frac{dN}{dt} = -(\alpha C + d)N \quad \text{(S60)}$$

The rate of pathogen introduction is designated as $\dot{m}$ (infective units/min, IU/min). The following equation shows the net change in number of pathogens as a function of both the introduction rate and removal rate:

$$\frac{dN}{dt} = \dot{m} - (\alpha C + d)N \quad \text{(S61)}$$

This equation can be integrated to get the number of pathogens, N, as shown in the following equation, that represents the time evolution of the number of pathogens assuming instant mixing (i.e., infinite diffusivity):

$$\mathrm{N} = \frac{\dot{m}}{\alpha C + d}\left(1 - e^{-(\alpha C + d)t}\right) \quad \text{(S62)}$$

For a steady-state condition at infinite time, the equation can be simplified to the following:

$$\mathrm{N} = \frac{\dot{m}}{\alpha C + d} \quad \text{(S63)}$$

Equation (S63) can be divided by the volume V on both sides to get a pathogen concentration P, and since P = N/V, the final Equation (9) in the main paper is written as the following:

$$P = \frac{\dot{m}/V}{\alpha C + d} \quad \text{(S64)}$$

S13.2. Transition Thresholds

The geometric series described in Section S10 becomes unstable and inaccurate when the ratio between the values in concentric rings (squares in the "Steady-State Pathogen Dose-Response Model" workbook "Diffusion Model" tab) approaches 1. It was empirically determined that the largest ratio with reasonable values was 0.83 when there was no "Velocity in x direction" component and was 0.90 when there was such a velocity. When these thresholds are exceeded, a #N/A result is intentionally produced in the workbook for that image plane and the macros that add results from image sources do not include such results. Also, when both image sides have #N/A, the image source summing is terminated. Distant image planes (i.e., the "z" direction) have higher ratios of the summed values of the concentric rings (in the "xy" plane) because the distance does not change very much due to the small angle between distant rings. While the geometric series projection error is higher, the contribution from such distant planes is usually small and an additional check described below ensures the overall result is reasonable.

The high ratio occurs when the diffusivity is high relative to the disinfection rate, in which case the solution approaches that of the well-mixed model. In order to determine when to transition to the well-mixed result, an error term is calculated in the macros when computing and summing the image sources where the change from the last real computed value (not #N/A) for an image plane must not change the sum result from all image planes by more than 0.1%. If it does or if no computation can be done at all (i.e., #N/A from the start), then the well-mixed model in Equation (S64) is used to calculate the average pathogen concentration. There is a limit of 100 image planes; so, if not terminated by an earlier #N/A, the error used is from the contribution of image plane 100.

One approaches the well-mixed model at higher diffusivity and slower disinfection rates. Slower disinfection rates can come from lower FC or higher CYA (i.e., lower HOCl) or from a slower to inactivate pathogen. At 2 ppm FC with 90 ppm CYA, switching to the well-mixed model occurs with a diffusivity above around 20,000,000 cm²/min for *E.coli*, 8,000 for *Giardia*, and 700 for *Cryptosporidium*.

S14. Distance Average and Annual Risk

The per-visit probability of infection is calculated in the model workbook using the distance parameters specified for the ingestor to the closest shedder. However, a distance average risk is also calculated by varying the horizontal position of the ingestor in the swimming pool and giving equal probability for all positions of an ingestor between infected bathers up to the specified closest distance. A grid of positions is used for the calculation, and to minimize error, the grid is aligned to have one point at the closest distance to a shedder on the diagonal between shedders.

The probability of infection is computed from the product of probabilities of not getting infected for a visit at each position. An effective distance average per-visit risk is calculated as shown in Equation (S65), and the annual risk is calculated as shown in Equation (S66).

$$DistanceAveragePerVisitRisk = 1 - \left(\prod_1^{GridCount}(1 - PerVisitPositionRisk_i)\right)^{\frac{1}{GridCount}} \quad \text{(S65)}$$

$$DistanceAverageAnnualRisk = 1 - (1 - DistanceAveragePerVisitRisk)^{VisitsPerYear} \quad \text{(S66)}$$

S15. Monochloramine Concentration Equivalent to HOCl in Model

Chlorine combines quickly with ammonia from sweat and urine to form monochloramine and more slowly forms dichloramine and nitrogen trichloride [49]. The model workbook has an informational tab "Monochloramine" that calculates the equivalent monochloramine concentration with equivalent disinfection to that from HOCl calculated from model inputs. Table S7 shows concentrations of monochloramine for the model pathogens for a few examples of model inputs.

Table S7. Concentration of monochloramine (mg/L Cl_2) equivalent in disinfection to HOCl.

Pathogen	CYA/FC = 90/2 = 45	CYA/FC = 80/4 = 20	FC = 1, no CYA
Escherichia coli O157 [50]	8.94×10^{-1}	2.09×10^{0}	5.01×10^{1}
Giardia [41]	2.63×10^{-1}	6.15×10^{-1}	1.37×10^{1}
Cryptosporidium parvum [51]	1.53×10^{-2}	3.58×10^{-2}	8.57×10^{-1}

The concentrations of monochloramine required to provide equivalent efficacy to HOCl when CYA is present show that the model assumption of treating HOCl as the sole disinfectant is valid for *Escherichia coli* O157 and likely valid for *Giardia* except possibly for conditions of a very high bather load. However, for *Cryptosporidium parvum*, monochloramine may play a significant role in disinfection because it has a Ct value (11,400) comparable to that of HOCl (15,300).

S16. Calculated HOCl from Swimming Pool Regulatory Codes

The ratio of highest to lowest HOCl concentrations allowed by State codes or guidelines that exceed 500 are shown in **bold**. There are 27 such states.

Table S8. Calculated HOCl concentrations from FC and CYA in regulatory codes for outdoor swimming pools: all values are in mg/L. FC and HOCl values are mg/L as Cl_2.

	Free Chlorine (FC)		Cyanuric Acid (CYA)		HOCl[i]		
State or Code	Low[a]	High	Low[a]	High	Lowest	Highest	Ref.
EPA	1.0[b]	4.0[g]	-	-	-	-	See notes
MAHC	1.0/2.0	10.0[h]	0	90	**0.00866**	**4.86**	[52]
Alabama (Montg.)	1.0	10.0	0	100	**0.00383**	**4.86**	[53]
Alaska	-	-	0	0	0.3[j]	-	[54]
Arizona	1.0	3.0	0	150	**0.00255**	**1.46**	[55]
Arkansas	1.0/1.5	5.0	0	90	0.00644	2.43	[56]
California	1.0/2.0	10.0	0	100	**0.00777**	**4.86**	[57] [58]
Colorado	0.25	5.0	20	100	0.000947	0.135	[59]
Connecticut	0.8/1.5	-	0	100	0.00579	-	[60]
Delaware	1.0/2.0	10.0	0	100	**0.00777**	**4.86**	[61]
District of Columbia	-	-	0	100			[62]
Florida	1.0	10.0	0	100	**0.00383**	**4.86**	[63]
Georgia	1.0	10.0	0	90	**0.00426**	**4.86**	[64]
Hawaii	0.6	-	-	-	-	-	[65]
Idaho	1.0	5.0	0	100	**0.00383**	**2.43**	[66]
Illinois	1.0[c]	4.0	0	100	**0.00383**	**1.94**	[67]
Indiana	1.0	7.0	0	60	**0.00641**	**3.40**	[68]
Iowa	1.0	8.0	0	80	**0.00479**	**3.89**	[69]
Kansas	1.0	5.0	-	-	-	2.43	[70]
Kentucky	1.0	2.5	0/25	50	**0.00771**	**1.21**	[71]
Louisiana	0.4	0.6	-	-	-	0.291	[72]
	1.0	10.0	0	90	**0.00866**	**4.86**	[73]
Maine	1.0	4.0	0	150	**0.00255**	**1.94**	[74]
Maryland	1.5	10.0	0/30	100	**0.00579**	**4.86**	[75]
Massachusetts	1.0	3.0	0/30	100	0.00383	1.46	[76]
Michigan	1.0/2.0[d]	-	0/20	80	0.00479	-	[77]
Minnesota	1.0	10.0	0	100	**0.00383**	**4.86**	[78]
Mississippi	1.0	3.0	-	-	-	1.46	[79]
Missouri (St. Louis)	2.0	8.0	0/10	100	0.00777	3.86	[80]
Montana	1.0	10.0	0	50	**0.00777**	**4.86**	[81]
Nebraska	2.0	-	0	50	0.0159	-	[82]
Nevada	1.0	5.0	0	100	**0.00383**	**2.43**	[83]
New Hampshire	1.0	5.0	0	50	0.00771	2.43	[84]
New Jersey	1.0	10.0	0/10	100	**0.00383**	**4.86**	[85]
New Mexico	1.0	5.0	0	100	**0.00383**	**2.43**	[86]
New York	0.6[e]	5.0	0	0	0.291	2.43	[87]
North Carolina	1.0	-	0	100	0.00383	-	[88]
North Dakota	1.0	-	-	-	-	-	[89]
Ohio	1.0	-	0	70	0.00548	-	[90]
Oklahoma	1.0	5.0	30	100	0.00383	0.0798	[91]
Oregon	1.5	5.0	0	150	**0.00384**	**2.43**	[92]
Pennsylvania	0.4	-	-	-	-	-	[93]
Rhode Island	1.0/2.0	10.0	0	25	0.0331	4.86	[94]
South Carolina	1.0	8.0	0	100	**0.00383**	**3.89**	[95]
South Dakota	1.0	-	-	-	-	-	[96]
Tennessee	0.5	3.0	0	100	**0.00190**	**1.46**	[97]
Texas	1.0	8.0	0	100	**0.00383**	**3.89**	[98]

Utah	1.0/2.0[f]	10.0	0	100	**0.00777**	**4.86**	[99]
Vermont	(no code found)		(no code found)				
Virginia	0.5	-	-	-	-	-	[100]
Washington	1.5/2.0	-	0	90	0.00866	-	[101]
West Virginia	1.0	5.0	0/10	100	**0.00383**	**2.43**	[102]
Wisconsin	1.0/1.5	10.0	0	30	0.0199	4.86	[103]
Wyoming	1.0	8.0	0	100	**0.00383**	**3.89**	[104]

[a] Where there are 2 numbers, the first is with no CYA while the second is with CYA.

[b] A minimum FC of 1.0 mg/L from OCSPP 810.2600 (formerly DIS/TSS-12), where AOAC 965.13 uses an NaOCl reference starting at 0.6 mg/L and not ending below 0.4 mg/L.

[c] An FC of 2.0 mg/L at 85 °F or higher.

[d] With CYA, FC is scaled adding 0.5 mg/L for every 20 mg/L CYA above 40 mg/L CYA, so the FC minimum is 3.0 mg/L at 80 mg/L CYA.

[e] An FC of 1.5 mg/L at or above a pH of 7.8.

[f] At or above a pH of 7.7, the FC minimum is 2.0/3.0.

[g] From national primary drinking water regulations with a Maximum Residual Disinfection Level (MRDL) for chlorine of 4.0 mg/L [105]: This is based on the No Observed Adverse Effect Limit (NOAEL) of 14.4 mg/kg-day in female rats exposed to chlorinated water for two years with an uncertainty factor of 100 (10 for interspecies and 10 for intraspecies variation). The drinking water equivalent level (DWEL) was calculated from (0.1 mg/kg/day) × (70 kg) / (2 L/day) = 3.5 mg/L ≅ 4 mg/L [106].

[h] MAHC says "FAC concentrations shall be consistent with label instructions", which would be 4.0 mg/L per EPA.

[i] At pH 7.5, temperature of 25 °C, and TDS 1000 mg/L.

[j] A table in the regulations of HOCl as a function of pH defines the minimum FC with no CYA allowed.

S17. Adjustments for Die-Off

The Chick–Watson equation with die-off (with "n" of 1) can be recast to show how experiments that do not account for natural die-off can be adjusted to show a linear plot of adjusted log reduction vs. Ct values:

$$ln(N_t/N_0) = -(\alpha C + d)t = -\alpha(Ct) - d \cdot t \quad \text{(S67)}$$

$$ln(N_t/N_0) + d \cdot t = -\alpha(Ct) \quad \text{(S68)}$$

Die-off becomes important when the chlorine disinfection rate is slow as it is with *Cryptosporidium*. The raw data from the experiments from Murphy [23] contained controls without chlorine from which the die-off rate (d) was calculated. This die-off constant was then multiplied by time and added to the raw log reduction for each data point based on Equation (S68).

S18. Disinfection Kinetics Results

The fact that HOCl is the primary active biocide in chlorine solutions without CYA has been well established for decades. In 1943, Butterfield [107] established that HOCl is a much more potent biocide than OCl^- and that most of the biocidal activity of chlorine is due to HOCl. Although not as well-established, this concept has also been proposed for chlorine solutions in the presence of CYA, that is, the various chlorinated isocyanurate compounds in solution have very little biocidal activity.

The idea that pathogen kill rates in the presence of CYA are directly proportional to HOCl concentrations has been proposed by Engel [22] in their work with *Naegleria gruberi*. Gardiner [108] also showed that the time required for a 99% kill of *S. faecalis* plotted versus the ratio of cyanuric acid:chlorine resulted in a straight line. Saita's [26] linear plots of survival ratios of poliovirus vs. the molar ratio of CYA:chlorine showed a similar relationship. Wahman [2] also argued "that the effective disinfectant in systems where chlorinated cyanurates are present is free chlorine, specifically HOCl". The work of Gardiner, Saita, Wahman, and Engel show that kill rates are proportional to the HOCl concentration in the presence of CYA.

To test the validity of this concept, data sets from the literature were evaluated for consistency with this assumption (see Supplemental workbook: "Literature calculations HOCl vs kill time.xlsx"). Unfortunately, few of the published studies provide the pathogen counts as a function of time. However, the Chick–Watson equation may be used to show that the proposal is consistent with a wide range of studies and organisms.

The Chick–Watson equation may be rearranged as follows:

$$ln(N_t/N_0) = -\alpha C^n t \quad \text{(S69)}$$

$$t = ln(N_t/N_0)/(\alpha C^n) \quad \text{(S70)}$$

Assuming a constant log reduction ($\ln(N_t/N_o)$), coefficient of lethality (α), and a dilution coefficient (n) of 1, a plot of contact time vs. 1/HOCl concentration should be linear if HOCl is responsible for most of the biocidal activity.

The supplemental workbooks "Literature calculations HOCl vs kill time.xlsx" and "Crypto Raw Data from CDC_122116 with calcs.xlsm" contain plots of contact time vs/ 1/HOCl and $\text{Log}(N/N_o)$ vs. Ct with data from various researchers.

Figure S4, using data from Murphy [23], shows that 3-log inactivation times correlate well with 1/HOCl concentration (correlation coefficient of 0.9957) and not with 1/FC concentration (correlation coefficient of 0.5871).

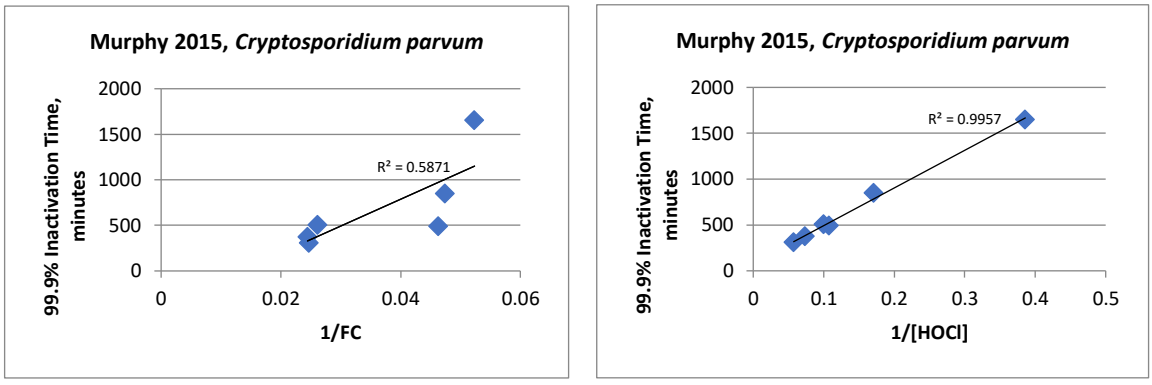

(**a**) (**b**)

Figure S4. Relationship between a *Cryptosporidium parvum* 99.9% inactivation time and (**a**) 1/FC and (**b**) 1/HOCl concentration in mg/L.

Although the relationships between $\text{Log}(N/N_o)$ vs Ct and inactivation time vs. 1/sanitizer concentration are complicated by many factors, the data from various researchers investigating various organisms show that HOCl concentrations are a better predictor of chlorine efficacy than FC concentrations.

S19. Selected Values for Model

The selected, minimum, and maximum values in Tables 6 and 7 are discussed below. The authors relied on data, codes, and standards when available as noted below. However, many of the minimum and maximum values were simply based on the experience and judgement of the authors. Some of the selected values were median values between two established limits (e.g., pH 7.5 is the median between the minimum and maximum pH values allowed in the *MAHC*). In other cases, there was no well-established minimum and maximum (e.g., distance between bathers), the median value would not be representative of current pools and practices (e.g., a 1.5-log secondary disinfection system), or there was a specific reason for choosing a value other than the median (e.g., FC 2 mg/L instead of 2.5 mg/L). Overall, the selected values are conservative for a typical commercial/public pool with a fairly high bather load and so may overestimate the risk of infection. However, the selected values likely underestimate the risk of infection from facilities defined by the Model Aquatic Health Code as "high risk venues" such as wading pools and splash pads.

S19.1. Table 6

FC 2 mg/L was chosen because it is the minimum chlorine concentration allowed in the *MAHC* for pools using CYA. It is also between the minimum residual requirement of 1 mg/L and the maximum limit of 4 mg/L prescribed by U.S. EPA for chlorine products used as biocides in swimming pools. The minimum value of 1 ppm is also the minimum prescribed in the *MAHC* for pools not using CYA. The maximum value of 10 ppm is from the *MAHC*.

CYA 90 mg/L was chosen because it is the maximum CYA level allowed in the *MAHC*. The maximum value of 100 ppm is consistent with many state health codes as well as guidance from the Association of Pool and Spa Professionals and other pool industry groups.

pH 7.5 was chosen as the mid-point between the minimum of 7.2 and maximum of 7.8 allowed in the *MAHC*.

A temperature of 25 °C was chosen because most of the kill rate studies were conducted at room temperature and 20–25 °C is typically considered room temperature for scientific studies. It should be noted that recommended pool temperatures vary depending on the activity, with the coolest recommendations for competitive pools of 26 °C [109] and maximum water temperatures up to 40 °C (104 °F maximum limit in *MAHC*). Furthermore, the O'Brien equilibrium constants were measured at 25 °C. Although 25 °C is cool for swimming, the low temperature has longer kill times and, so, is a more conservative approach.

TDS 1,000 mg/L was chosen as a round figure that would be reasonable for many swimming pools. The Association of Pool and Spa Professionals American National Standard for Water Quality in Public Pools and Spas [110] recommends that pools be drained if the TDS concentration increases greater than 1,500 mg/L over the concentration from when the pool was first filled. The minimum and maximum values of 500 and 5,000 mg/L were chosen to span an order of magnitude, with the minimum being a reasonable value for a freshly filled pool that has been adjusted for water balance and the maximum being a high value for a pool that uses an electrolytic chlorine generator.

Secondary disinfection per pass 99.9% was chosen as both the selected and maximum values because the *MAHC* requires secondary disinfection systems to achieve a minimum 3-log reduction in the number of infective *Cryptosporidium parvum* oocysts per pass through the secondary disinfection system for interactive water play aquatic venues: 90% was chosen as the minimum value because some filters may be capable of a 1-log removal of pathogens [111].

Secondary disinfection turnover time of 0 minutes was chosen, even though it is lower than the minimum value, because most swimming pools are not required by the *MAHC* to have secondary disinfection systems (and 0 in the model disables secondary disinfection). For the purposes of this paper, to evaluate the effect of CYA, secondary disinfection was not included. This function was incorporated into the model as a tool for researchers, regulators, and operators to use when

calculating predicted risks for facilities with secondary disinfection. The minimum and maximum values of 30 and 360 minutes span the minimum and maximum turnover times in the *MAHC* for most pools. The only exception is the 8-hour turnover time allowed for diving pools.

Water replacement rate of 0 L/bather was chosen to keep the model as simple as possible. Like secondary disinfection, this function was incorporated as a tool for future use of the model. The maximum 30 L/bather is taken from WHO recommendations [112].

Diffusivity 500 cm^2/min (0.54 ft^2/min) in the xy plane was chosen because turbulent diffusion is typically in the hundreds to thousands of cm^2/min. Setting this value to 500 cm^2/min results in D_x and D_y from Equations (6)–(8) in the main paper being equal to 500 cm^2/min. At 500 cm^2/min, the time for an instantaneous point release to reach the maximum concentration at the ingestion point with no disinfection is about 1 ½ minutes.

Diffusivity in the vertical direction (D_z) was chosen to be the same as the xy diffusivity (i.e., 100% results in D_z being equal to D_x and D_y).

Velocity of 0 cm/min in the x direction (U_x) was chosen to keep the model as simple as possible. Future use of the model may choose to simulate one swimmer swimming behind another or bathers in a unidirectional flow. For example, the velocity of a swimmer capable of swimming 25 yards in 30 seconds would have a velocity of 4572 cm/min. Trained competitive swimmers achieve speeds around 4 miles/hour (10,000 cm/min).

Depth of pool at 91.44 cm is a typical shallow pool depth of 3 feet. This value is used for the boundary conditions described in main paper Section 2.4.3. The minimum and maximum values of 30.48 cm and 250 cm represent 1 ft. and 8.2 ft., respectively.

Distance between bathers 118.05 cm (3.87 ft.) is equivalent to 15 ft^2/bather of surface area. The *MAHC* specifies a peak occupancy of 20 ft^2/bather for flat water and 15 ft^2/bather for agitated water. The minimum value of 80 cm (2.62 ft.) is equivalent to 6.9 ft^2/bather, and 240 cm (7.87 ft) is equivalent to 62 ft^2/bather.

The ingestion to source plane (45.72 cm), x distance to source (45.72 cm), y distance to source (0 cm), and source plane height (45.72 cm) settings will result in the $x–x_o$ and $z–z_o$ distances being 45.72 cm (1.5 ft) and $y–y_o$ being 0 cm. This distance is half the 3 ft pool depth. In choosing this value, the mean height of children in the United States was also considered [113].

Ingestion rate of 24.2 ml/hr was chosen because it is the mean pool water ingestion rate for children from Suppes [114]. The mean ingestion rate for adults is 6.3 ml/hr [114]. Suppes reported a range of 0–60.6 ml/hr for adults and 0–105.5 ml/hr for children.

Exposure time 1.9 hrs/visit was chosen because it is the mean swim duration for children from Suppes [114]. The mean swim duration for adults is 1.2 hrs/visit [114]. Suppes reported a range of 0.3–4 h for adults and 0.5–8 h for children.

Exposure frequency of 72.9 visits/year was chosen because it is the mean visit frequency for children from Suppes. The mean visit frequency for all swimmers is 72.6 visits/yr [114]. Suppes reported a range of 1–360 visits/yr for adults and 1–200 visits/yr for children.

Fecal introduction rate of 0.0007 g/bather/min was chosen because it is the mean fecal shedding rate calculated from Keuten et al. [115]. If the Gerba data [116] for children is used (mean 21.1 mg/bather/min and maximum 667 mg/bather/min), extraordinarily high risk predictions result from the model. In order to evaluate the other input parameters, a more moderate fecal introduction rate was used for the selected value. The Keuten values may also be more realistic since they are based on pool-side shower data from 32 adults and one child. The Gerba data included household shower data of families with small children 18 months to 9 years. The calculation of the minimum (0.04 mg/bather/min) and maximum (667 mg/bather/min) values are discussed in the main paper Section 2.4.1 and are the minimum and maximum values from Table 2.

S19.2. Table 7

The selected values in Table 7 are discussed in the relevant sections of the main paper:
%Infected: Section 2.4.3

Inactivation rate: Section 2.4.2

Die-off rate: Section 2.4.2

Dose response: Section 2.4.4

When the minimum percent infected values are set to 0%, the model calculates the risk of infection for bathers swimming next to a single infected bather.

The minimum *E. coli* inactivation rate is from Zhao et al. [117], where one of the strains tested was more resistant to chlorine.

The maximum *E. coli* inactivation rate is from Table 3.1 in LeChevalier and Kwok-Keung [118].

The minimum and maximum inactivation rates for *Giardia* and *Cryptosporidium* were taken as ½ the selected value and 2 times the selected value, respectively.

The die-off rate minimums for all three pathogens were set to zero to see the effect of not including this parameter.

The maximum *E. coli* and *Giardia* die-off rates were chosen to be 2x the selected values. The maximum *Cryptosporidium* die off rate is from Murphy [23].

The dose response minimums and maximums used in the sensitivity analysis were the 5th and 95th percentiles, respectively, for *E. coli* [119], *Giardia* [120], and *Cryptosporidium* [121].

S20. Accidental Fecal Release (AFR)

According to Hlavsa et al. [122], from 2000–2014, 42% of outbreaks and 79% of cases in treated recreational water were from the parasite *Cryptosporidium* while only 2% of outbreaks and 1% of cases were from the parasite *Giardia*. The model described in the main paper shows the higher risk from regular fecal sloughing in high bather-load pools to be from *Giardia*. The difference may be due to outbreaks being caused not by regular fecal sloughing but by an accidental fecal release (AFR).

An AFR, particularly from diarrhea, is a much larger volume of fecal matter dispersed in the water in a much shorter period of time. According to Rendtoff and Kashgarian [123], the average weight of a stool is 123.6 g, but diarrhea stool volumes can exceed 2 L in immunocompromised patients [124]. By comparison, regular fecal sloughing is on the order of 20 mg/hour to 100 mg/hour (or 0.5 to 18 g/hour using young children data from Gerba).

Also according to Rendtorff and Kashgarian [123], volunteers fed *C. parvum* who developed diarrhea had over 10 times the oocyst concentration in their stools than those without diarrhea. Regular fecal sloughing in this paper assumed oocyst concentration in infected individuals consistent with those without diarrhea.

With an AFR, the faster chlorine disinfection of *Giardia* vs. *Cryptosporidium* may limit outbreaks to a single day. A model for AFRs can be developed and will be examined in a future paper.

S21. Monochloramine Comparison

The calculations may be found in "Monochloramine comparison.xlsx" [125–127].

References

1. O'Brien, J.E.; Morris, J.C.; Butler, J.N. Equilibria In Aqueous Solutions of Chlorinated Isocyanurate. In Chemistry of Water Supply, Treatment, and Distribution; Rubin, A.J., Ed.; Ann Arbor Science Publishers: Ann Arbor, 1974; pp. 333–358 ISBN 0-250-40036-7.

2. Wahman, D.G. Chlorinated Cyanurates: Review of Water Chemistry and Associated Drinking Water Implications. J. AWWA 2018, 110(9), 1–15.

3. Malmburg, C.G.; Maryott, A.A. Dielectric Constant of Water from 0 to 100 C. J. Res. Natl. Bur. Stand. (1934). 1956, 56(1), 1–8.

4. O'Brien, J.E. Hydrolytic and Ionization Equilibria of Chlorinated Isocyanurate in Water, Harvard University, 1972.

5. Langelier, W.F. The Analytical Control of Anti-Corrosion Water Treatment. J. Am. Water Works Assoc. 1936, 28(10), 1500–1521.
6. Schock, M.R. Temperature and Ionic Strength Corrections to the Langelier Index—Revisited. J. Am. Water Works Assoc. 1984, 76(8), 72–76.
7. Lewis, G.N.; Randall, M. The Activity Coefficient of Strong Electrolytes. J. Am. Chem. Soc. 1921, 43(5), 1112–1154.
8. Morris, J.C. The Acid Ionization Constant of HOCl from 5 to 35°. J. Phys. Chem. 1966, 70(12), 3798–3805.
9. Wojtowicz, J.A. Reevaluation of Chloroisocyanurate Hydrolysis Constants. J. Swim. Pool Spa Ind. 2001, 2(2), 14–22.
10. Pinsky, M.L.; Hu, H.-C. Evaluation of the chloroisocyanurate hydrolysis constants. Environ. Sci. Technol. 1981, 15(4), 423–430.
11. Solastiouk, B. Thermodynamic and kinetic study of the chlorine / cyanuric acid system in aqueous solution, Lorraine National Polytechnic Institute, Nancy, France, 1989.
12. Wahman, D.G. First acid ionization constant of the drinking water relevant chemical cyanuric acid from 5 to 35 °C. Environ. Sci. Water Res. Technol. 2018, 4, 1522–1530.
13. Wahman, D.G.; Alexander, M.T. A Drinking Water Relevant Water Chemistry Model for the Free Chlorine and Cyanuric Acid System from 5°C to 35°C. Environ. Eng. Sci. 2019, 36(3), 283–294.
14. Andersen, J.R. The influence of cyanuric acid on the bactericidal effectiveness of chlorine, University of Wisconsin, 1963.
15. Andersen, J.R. A Study of the Influence of Cyanuric Acid on the Bactericidal Effectiveness of Chlorine. Am. J. Public Health 1965, 55(10), 1629–1637.
16. Fitzgerald, G.P.; DerVartanian, M.E. Factors Influencing the Effectiveness of Swimming Pool Bactericides. Appl. Microbiol. 1967, 15(3), 504–509.
17. Fitzgerald, G.P.; DerVartanian, M.E. Pseudomonas aeruginosa for the evaluation of swimming pool chlorination and algicides. Appl Microbiol 1969, 17(3), 415–421.
18. Golaszewski, G.; Seux, R. The Kinetics of the Action of Chloroisocyanurates on Three Bacteria: Pseudomonas aeruginosa, Streptococcus faecalis and Staphylococcus aureus. Water Res. 1994, 28(1), 207–217.
19. Robinton, E.D.; Mood, E.W. An evaluation of the inhibitory influence of cyanuric acid upon swimming pool disinfection. Am. J. Public Health Nations. Health 1967, 57(2), 301–10.
20. van Klingeren, B.; Pullen, W.; Reijnders, H.F. Quantitative suspension test for the evaluation of disinfectants for swimming pool water: experiences with sodium hypochlorite and sodium dichloroisocyanurate. Zentralbl. Bakteriol. B. 1980, 170(5–6), 457–68.
21. Victorin, K.; Hellström, K.G.; Rylander, R. Redox potential measurements for determining the disinfecting power of chlorinated water. J. Hyg. (Lond). 1972, 70(2), 313–23.
22. Engel, J.P.; Rubin, A.J.; Sproul, O.J. Inactivation of Naegleria gruberi cysts by Chlorinated Cyanurates. Appl. Environ. Microbiol. 1983, 46(5), 1157–1162.
23. Murphy, J.L.; Arrowood, M.J.; Lu, X.; Hlavsa, M.C.; Beach, M.J.; Hill, V.R. Effect of Cyanuric Acid on the Inactivation of Cryptosporidium parvum under Hyperchlorination Conditions. Environ. Sci. Technol. 2015, 49(12), 7348–7355.
24. Shields, J.M.; Arrowood, M.J.; Hill, V.R.; Beach, M.J. The effect of cyanuric acid on the disinfection rate of Cryptosporidium parvum in 20-ppm free chlorine. J. Water Health 2009, 7(1), 109–114.
25. Sommerfeld, M.R.; Adamson, R.P. Influence of stabilizer concentration on effectiveness of chlorine as an algicide. Appl. Environ. Microbiol. 1982, 43(2), 497–499.
26. Saita, K.; Tachikawa, M.; Tezuka, M.; Sawamura, R. Effects of Isocyanuric Acid on the Poliovirus Inactivation with Hypochlorous Acid. Japan J. Toxicol. Environ. Heal. 1998, 44(6), 442–450.
27. Tachikawa, M.; Saita, K.; Ryoji, S. Inactivation of Poliovirus with Chlorine Compounds and Effects of Chloramine Formation (Proceedings of the 20th Symposium on Toxicology and Environmental Health). Eisei kagaku 1995, 41(1), P6–P6.
28. Yamashita, T.; Sakae, K.; Ishihara, Y.; Isomura, S.; Inoue, H. Virucidal effect of chlorinated water containing cyanuric acid. Epidemiol. Infect. 1988, 101(3), 631–639.
29. Yamashita, T.; Sakae, K.; Ishihara, Y.; Inoue, H.; Isomura, S. [Influence of cyanuric acid on virucidal effect of chlorine and the comparative study in actual swimming pool waters]. Kansenshogaku Zasshi. 1988, 62(3), 200–5.

30. Yamashita, T.; Sakae, K.; Ishihara, Y.; Isomura, S.; Takeuchi, K. [Microbiological and chemical analyses of indoor swimming pools and virucidal effect of chlorine in these waters]. Nihon. Koshu Eisei Zasshi. 1990, 37(12), 962–6.
31. Black, A.P.; Keirn, M.A.; Smith, Jr., J.U.; Dykes, G.M.; Harlan, W.E. The Disinfection of Swimming Pool Water Part II. A Field Study of the Disinfection of Public Swimming Pools. Am. J. Public Health 1970, 60(4), 740–750.
32. Esterman, A.; Roder, D.M.; Cameron, A.S.; Robinson, B.S.; Walters, R.P.; Lake, J.A.; Christy, P.E. Determinants of the microbiological characteristics of South Australian swimming pools. Appl. Environ. Microbiol. 1984, 47(2), 325–8.
33. Favero, M.S.; Drake, C.H.; Randall, G.B. Use of Staphylococci as Indicators of Swimming Pool Pollution. Public Health Rep. 1964, 79(1), 61–70.
34. Kowalski, X.; Hilton, T.B. Comparison of Chlorinated Cyanurates With Other Chlorine Disinfectants. Public Health Rep. 1966, 81(3), 282–288.
35. LeGuyader, M.; Grateloup, I. Relative importance of different bacteriological parameters in swimming pool water treated by hypochlorite or chloroisocyanurates. J. Fr. d'Hydrologie 1988, 19(2), 241–250.
36. APSP Recreational Water Quality Committee (RWQC) Bromine 2017, 1–4.
37. Yang, S.; McCoy, W.F. Sunlight-ultraviolet-stable biocide compositions and uses thereof in water treatment 1999.
38. Elmir, S.M.; Wright, M.E.; Abdelzaher, A.; Solo-Gabriele, H.M.; Fleming, L.E.; Miller, G.; Rybolowik, M.; Shih, M.-T.P.; Pillai, S.P.; Cooper, J.A.; et al. Quantitative evaluation of bacteria released by bathers in a marine water. Water Res. 2007, 41(1), 3–10.
39. Zubrzycki, L.; Spaulding, E.H. Studies on the Stability of the Normal Human Fecal Flora. J. Bacteriol. 1962, 83(5), 968–974.
40. Karch, H.; Rüssmann, H.; Schmidt, H.; Schwarzkopf, A.; Hessemann, J. Long-Term Shedding and Clonal Turnover of Enterohemorrhagic Escherichia coli O157 in Diarrheal Diseases. J Clin Microbiol. 1995, 33(6), 1602–1605.
41. U.S. EPA LT1ESWTR Disinfection Profiling and Benchmarking Technical Guidance Manual.; 2003;
42. Gage, S.D.; Ferguson, H.F.; Gillespie, C.G.; Messer, R.; Tisdale, E.S.; Hinman, J.J.; Green, H.W. Swimming Pools and Other Public Bathing Places. Am. J. Public Health 1926, 16(12), 1186–1201.
43. Socolofsky, S.A.; Jirka, G.H. Environmental Fluid Mechanics Part I: Mass Transfer and Diffusion; Engineering Lectures Available online: http://www.ifh.uni-karlsruhe.de/lehre/envflu_I/Downloads/course_script/ed2/script_ed2.pdf.
44. Majowicz, S.E.; Scallan, E.; Jones-Bitton, A.; Sargeant, J.M.; Stapleton, J.; Angulo, F.J.; Yeung, D.H.; Kirk, M.D. Global incidence of human Shiga toxin-producing Escherichia coli infections and deaths: a systematic review and knowledge synthesis. Foodborne Pathog. Dis. 2014, 11 (6), 447–455.
45. Scallan, E.; Hoekstra, R.M.; Angulo, F.J.; Tauxe, R. V.; Widdowson, M.A.; Roy, S.L.; Jones, J.L.; Griffin, P.M. Foodborne illness acquired in the United States-Major pathogens. Emerg. Infect. Dis. 2011, 17(1), 7–15.
46. CDC Prevalence of parasites in fecal material from chlorinated swimming pools--United States, 1999. Morb. Mortal. Wkly. Rep. 2001, 50(20), 410–412.
47. Hellard, M.E.; Sinclair, M.I.; Hogg, G.G.; Fairley, C.K. Prevalence of enteric pathogens among community based asymptomatic individuals. J. Gastroenterol. Hepatol. 2000, 15(3), 290–293.
48. Furness, B.W.; Beach, M.J.; Roberts, J.M. Giardiasis Surveillance --- United States, 1992--1997. Morb. Mortal. Wkly. Rep. Surveill. Summ. 2000, 49(SS07), 1–13.
49. Jafvert, C.T.; Valentine, R.L. Reaction Scheme for the Chlorination of Ammoniacal Water. Environ. Sci. Technol. 1992, 26 (3), 577–586.
50. Chauret, C.; Smith, C.; Baribeau, H. Inactivation of Nitrosomonas europaea and pathogenic Escherichia coli by chlorine and monochloramine. J. Water Health 2008, 6 (3), 315–322.
51. Driedger, A.M.; Rennecker, J.L.; Mariñas, B.J. Inactivation of Cryptosporidium parvum oocysts with ozone and monochloramine at low temperature. Water Res. 2001, 35 (1), 41–48.
52. CDC Model Aquatic Health Code, 3rd Edition Available online: https://www.cdc.gov/mahc/index.html (accessed on Jun 23, 2019).

53. County Code Montgomery AL Available online: https://www.alabamapublichealth.gov/montgomery/assets/2018MONTGOMERYCOUNTYPOOLRULES.pdf (accessed on Jun 23, 2019).
54. State Code AK Available online: http://www.akleg.gov/basis/aac.asp#18.30.550 (accessed on Jun 23, 2019).
55. State Code AZ Available online: https://apps.azsos.gov/public_services/Title_18/18-05.pdf (accessed on Jun 23, 2019).
56. State Code AR Available online: https://www.healthy.arkansas.gov/images/uploads/rules/SwimmingPools1.pdf (accessed on Jun 23, 2019).
57. State Code CA FC Available online: https://govt.westlaw.com/calregs/Document/IA66BDDEE3F5049318A33F8CB202AA97B (accessed on Jun 23, 2019).
58. State Code CA CYA Available online: https://govt.westlaw.com/calregs/Document/I8EA4216A7ACC43FDA2583D74C9616821 (accessed on Jun 23, 2019).
59. State Code CO Available online: https://www.sos.state.co.us/CCR/GenerateRulePdf.do?ruleVersionId=375&fileName=5 CCR 1003-5 (accessed on Jun 23, 2019).
60. State Code CT Available online: https://portal.ct.gov/-/media/Departments-and-Agencies/DPH/dph/environmental_health/recreation/pdf/1913b33bpdf.pdf?la=en (accessed on Jun 23, 2019).
61. State Code DE Available online: http://regulations.delaware.gov/AdminCode/title16/Department of Health and Social Services/Division of Public Health/Health Systems Protection (HSP)/4464.pdf (accessed on Jun 23, 2019).
62. State Code DC Available online: https://doh.dc.gov/sites/default/files/dc/sites/doh/publication/attachments/Pool Reg Title 22 Chap 64 - old_0.pdf (accessed on Jun 23, 2019).
63. State Code FL Available online: https://www.flrules.org/Gateway/View_notice.asp?id=17729095 (accessed on Jun 23, 2019).
64. State Code GA Available online: https://dph.georgia.gov/sites/dph.georgia.gov/files/EnvHealth/Pools/EnvHealthPoolsChapter511-3-5New.pdf (accessed on Jun 23, 2019).
65. State Code HI Available online: http://health.hawaii.gov/san/files/2013/05/11-10.pdf (accessed on Jun 23, 2019).
66. State Code ID Available online: https://adminrules.idaho.gov/rules/current/16/160214.pdf (accessed on Jun 23, 2019).
67. State Code IL Available online: http://www.ilga.gov/commission/jcar/admincode/077/077008200D03200R.html (accessed on Jun 23, 2019).
68. State Code IN Available online: https://www.in.gov/isdh/files/410_iac_6_2_1.pdf (accessed on Jun 23, 2019).
69. State Code IA Available online: http://idph.iowa.gov/Portals/1/Files/SwimmingPoolsandSpas/641-Chapter 15 Swimming Pools and Spas.pdf (accessed on Jun 23, 2019).
70. State Code KS Available online: https://library.municode.com/ks/wichita/codes/code_of_ordinances?nodeId=TIT7PUHE_CH7.72SWPO_S7.72.120DIMAMEWAQUST (accessed on Jun 23, 2019).
71. State Code KY Available online: https://apps.legislature.ky.gov/law/kar/902/010/120.pdf (accessed on Jun 23, 2019).
72. State Code LA - Title 51 Available online: https://www.doa.la.gov/pages/osr/lac/books.aspx (accessed on Jun 23, 2019).
73. Letter of Intent LA Available online: http://ldh.la.gov/assets/oph/Center-EH/engineering/LOI/LOI-Water_Quality_Parameters_in_Public_Swimming_Pools.pdf (accessed on Jun 23, 2019).
74. State Code ME Available online: https://www.maine.gov/sos/cec/rules/10/144/144c202.doc (accessed on Jun 23, 2019).
75. State Code MD Available online: http://www.dsd.state.md.us/comar/comarhtml/10/10.17.01.44.htm (accessed on Jun 23, 2019).

76. State Code MA Available online: https://www.mass.gov/files/documents/2016/07/qa/105cmr435_0.pdf (accessed on Jun 23, 2019).
77. State Code MI Available online: https://www.michigan.gov/documents/deq/deq-wb-dwehs-sp-mor_254923_7.pdf (accessed on Jun 23, 2019).
78. State Code MN Available online: https://www.revisor.mn.gov/rules/4717.1750/ (accessed on Jun 23, 2019).
79. State Guidelines MS Available online: http://www.msdh.state.ms.us/msdhsite/_static/resources/144.pdf (accessed on Jun 23, 2019).
80. State Code MO Available online: https://stlouisco.com/Portals/8/docs/Health/SwimmingPool/POOL CODE RULES REGS.pdf (accessed on Jun 23, 2019).
81. State Code MT Available online: https://dphhs.mt.gov/Portals/85/publichealth/documents/FCS/CircularFCS3_2018.pdf?ver=2018-10-23-151346-937 (accessed on Jun 23, 2019).
82. State Code NE Available online: http://www.sos.ne.gov/rules-and-regs/regsearch/Rules/Health_and_Human_Services_System/Title-178/Chapter-02.pdf (accessed on Jun 23, 2019).
83. State Code NV Available online: https://www.leg.state.nv.us/nac/nac-444.html#NAC444Sec148 (accessed on Jun 23, 2019).
84. State Code NH Available online: https://www.des.nh.gov/organization/commissioner/legal/rules/documents/env-wq1100.pdf (accessed on Jun 23, 2019).
85. State Code NJ Available online: https://www.state.nj.us/health/ceohs/documents/phss/recbathing.pdf (accessed on Jun 23, 2019).
86. State Code NM Available online: https://www.env.nm.gov/fod/Swim_Pools/pdfs/7.18.4 NMACFinal.pdf (accessed on Jun 23, 2019).
87. State Code NY Available online: https://www.health.ny.gov/regulations/nycrr/title_10/part_6/subpart_6-1.htm#s6111 (accessed on Jun 23, 2019).
88. State Code NC Available online: https://ehs.ncpublichealth.com/docs/rules/294306-9-2500.pdf (accessed on Jun 23, 2019).
89. State Code ND Available online: https://www.legis.nd.gov/information/acdata/pdf/33-29-01.pdf (accessed on Jun 23, 2019).
90. State Code OH Available online: http://codes.ohio.gov/oac/3701-31-04 (accessed on Jun 23, 2019).
91. State Code OK Available online: https://www.ok.gov/health2/documents/Public Bathing Places320.pdf (accessed on Jun 23, 2019).
92. State Code OR Available online: https://www.oregon.gov/oha/ph/healthyenvironments/recreation/poolslodging/documents/sparules.pdf (accessed on Jun 23, 2019).
93. State Code PA Available online: https://www.pacode.com/secure/data/028/chapter18/s18.29.html (accessed on Jun 23, 2019).
94. State Code RI Available online: https://risos-apa-production-public.s3.amazonaws.com/DOH/REG_9319_20180811132259.pdf (accessed on Jun 23, 2019).
95. State Code SC Available online: https://live-sc-dhec.pantheonsite.io/sites/default/files/media/document/R.61-51.pdf (accessed on Jun 23, 2019).
96. State Code SD Available online: http://denr.sd.gov/des/dw/PDF/Swimming Pool Management Manual.pdf (accessed on Jun 23, 2019).
97. State Code TN Available online: https://www.tn.gov/content/dam/tn/health/documents/1200-23-05.pdf (accessed on Jun 23, 2019).
98. State Code TX Available online: https://texreg.sos.state.tx.us/fids/25_0265_0204-4.html (accessed on Jun 23, 2019).
99. State Code UT Available online: https://rules.utah.gov/publicat/code/r392/r392-302.htm#T27 (accessed on Jun 23, 2019).
100. State Code VA Available online: http://www.vdh.virginia.gov/content/uploads/sites/91/2016/06/swimming.pdf (accessed on Jun 23, 2019).

101. State Code WA Available online: https://apps.leg.wa.gov/WAC/default.aspx?cite=246-260-999 (accessed on Jun 23, 2019).
102. State Code WV Available online: http://apps.sos.wv.gov/adlaw/csr/readfile.aspx?DocId=8316&Format=PDF (accessed on Jun 23, 2019).
103. State Code WI Available online: http://docs.legis.wisconsin.gov/code/admin_code/atcp/055/76/II/16 (accessed on Jun 23, 2019).
104. State Code WY Available online: http://agriculture.wy.gov/images/stories/pdf/chs/poolregs/chapter5.pdf (accessed on Jun 23, 2019).
105. U.S. EPA National Primary Drinking Water Regulations (NPDWR) Available online: https://www.epa.gov/sites/production/files/2016-06/documents/npwdr_complete_table.pdf.
106. U.S. EPA Reregistration Eligibility Decision (RED); Chlorine Gas Available online: https://archive.epa.gov/pesticides/reregistration/web/pdf/4022red.pdf (accessed on Jun 23, 2019).
107. Butterfield, C.T.; Wattie, E.; Megregian, S.; Chambers, C.W. Influence of pH and Temperature on the Survival of Coliforms and Enteric Pathogens When Exposed to Free Chlorine. Public Heal. Reports 1943, 58(51), 1837–1866.
108. Gardiner, J. Chloroisocyanurates in the treatment of swimming pool water. Water Res. 1973, 7(6), 823–833.
109. FINA FINA Facilities Rules 2017, 1–38.
110. APSP ANSI/APSP-11 2009: American National Standard for Water Quality in Public Pools and Spas 2009, 1–62.
111. Lu, P.; Amburgey, J.E.; Hill, V.R.; Murphy, J.L.; Schneeberger, C.; Arrowood, M.J. A full-scale study of Cryptosporidium parvum oocyst and Cryptosporidium-sized microsphere removals from swimming pools via sand filtration. Water Qual. Res. J. 2017, 52(1), 18–25.
112. World Health Organization Guidelines for safe recreational water environments - Volume 2: Swimming pools and similar environments; 2006;
113. Fryar, C.D.; Gu, Q.; Ogden, C.L.; Flegal, K.M. Anthropometric reference data for children and adults: United States, 2011–2014. Natl. Cent. Heal. Stat. Vital Heal. Stat. 2016, 3(39), 1–46.
114. Suppes, L.M.; Canales, R.A.; Gerba, C.P.; Reynolds, K.A. Cryptosporidium risk from swimming pool exposures. Int. J. Hyg. Environ. Health 2016, 219(8), 915–919.
115. Keuten, M.G.A.; Schets, F.M.; Schijven, J.F.; Verberk, J.Q.J.C.; van Dijk, J.C. Definition and quantification of initial anthropogenic pollutant release in swimming pools. Water Res. 2012, 46(11), 3682–3692.
116. Gerba, C.P. Assessment of enteric pathogen shedding by bathers during recreational activity and its impact on water quality. Quant. Microbiol. 2000, 2 (1), 55–68.
117. Zhao, T.; Doyle, M.P.; Zhao, P.; Blake, P.; Wu, F.-M. Chlorine inactivation of Escherichia coli O157:H7 in water. J. Food Prot. 2001, 64(10), 1607–1609.
118. LeChevalier, M.W.; Kwok-Keung, A. Water treatment and pathogen control: Process efficiency in achieving safe drinking water 2004, 1–112.
119. Cornick, N.A.; Helgerson, A.F. Transmission and Infectious Dose of Escherichia coli O157 : H7 in Swine. Appl. Environ. Microbiol. 2004, 70(9), 5331–5335.
120. Rendtorff, R.C. The Experimental Transmission of Human Intestinal Protozoan Parasites II. Giardia Lamblia Cysts Given in Capsules. Am. J. Epidemiol. 1954, 59(2), 209–222.
121. Messner, M.J.; Chappell, C.L.; Okhuysen, P.C. Risk Assessment for Cryptosporidium: A Hierarchical Bayesian Analysis of Human Dose Response Data. Water Res. 2001, 35(16), 3934–3940.
122. Hlavsa, M.C.; Cikesh, B.L.; Roberts, V.A.; Kahler, A.M.; Vigar, M.; Hilborn, E.D.; Wade, T.J.; Roellig, D.M.; Murphy, J.L.; Xiao, L.; et al. Outbreaks Associated with Treated Recreational Water — United States, 2000 – 2014. Morb. Mortal. Wkly. Rep. 2018, 67(19), 547–551.
123. Rendtorff, R.C.; Kashgarian, M. Stool patterns of healthy adult males. Dis. Colon Rectum 1967, 10(3), 222–228.
124. Leitch, G.J.; He, Q. Cryptosporidiosis-an overview. J. Biomed. Res. 2012, 25(1), 1–16.
125. O'Connell, H.A.; Rose, L.J.; Shams, A.; Bradley, M.; Arduino, M.J.; Rice, E.W. Variability of Burkholderia pseudomallei strain sensitivities to chlorine disinfection. Appl. Environ. Microbiol. 2009, 75(16), 5405–5409.
126. Rose, L.J.; Rice, E.W.; Jensen, B.; Murga, R.; Peterson, A.; Donlan, R.M.; Arduino, M.J. Chlorine inactivation of bacterial bioterrorism agents. Appl. Environ. Microbiol. 2005, 71(1), 566–568.

127. Rose, L.J.; Rice, E.W.; Hodges, L.; Peterson, A.; Arduino, M.J. Monochloramine inactivation of bacterial select agents. Appl. Environ. Microbiol. 2007, 73(10), 3437–3439.